BIOCHEMISTRY
including biophysical chemistry & molecular biology

Current Topic

pubs.acs.org/biochemistry

Designing Hydrolytic Zinc Metalloenzymes

Melissa L. Zastrow[†] and Vincent L. Pecoraro*

Department of Chemistry, University of Michigan, Ann Arbor, Michigan 48109, United States

ABSTRACT: Zinc is an essential element required for the function of more than 300 enzymes spanning all classes. Despite years of dedicated study, questions regarding the connections between primary and secondary metal ligands and protein structure and function remain unanswered, despite numerous mechanistic, structural, biochemical, and synthetic model studies. Protein design is a powerful strategy for reproducing native metal sites that may be applied to answering some of these questions and subsequently generating novel zinc enzymes. From examination of the earliest design studies introducing simple Zn(II)-binding sites into de novo and natural protein scaffolds to current studies involving the preparation of efficient hydrolytic zinc sites, it is increasingly likely that protein design will achieve reaction rates previously thought possible only for native enzymes. This Current Topic will review the design and redesign of Zn(II)-binding sites in de novo-designed proteins and native protein scaffolds toward the preparation of catalytic hydrolytic sites. After discussing the preparation of Zn(II)-binding sites in various scaffolds, we will describe relevant examples for reengineering existing zinc sites to generate new or altered catalytic activities. Then, we will describe our work on the preparation of a de novo-designed hydrolytic zinc site in detail and present comparisons to related designed zinc sites. Collectively, these studies demonstrate the significant progress being made toward building zinc metalloenzymes from the bottom up.

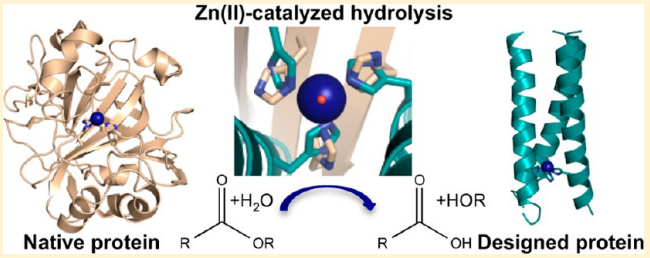

Zinc is an essential cofactor in thousands of proteins. As one of the most prevalent transition metal cofactors in biological systems, it plays structural, signaling, and regulatory roles and is found in all six classes of enzymes (most commonly hydrolases).[1,2] The discovery of its presence as the catalytic center in the hydrolytic metalloenzyme carbonic anhydrase (CA) in 1939[3] was followed by its characterization in carboxypeptidase in 1950[4] and, soon after, in enzymes of all classes.[5] In 1990, Vallee and Auld published a report analyzing the coordination spheres around Zn(II) in available protein crystal structures, including examples from most of the enzyme classes.[6] Here, the authors introduced the spacer rule for native zinc proteins, in which at least two of the ligating residues exist within a few residues (1−3) of each other in the primary sequence, while the third is separated by a longer spacer much more varied in length (5−200 residues). This rule, in which the shorter spacer is proposed as a nucleus for formation of the Zn(II) site while the longer spacer allows for some flexibility, has been rarely violated. The general guidelines for the coordination of Zn(II) in proteins have been described in a number of reports.[2,7] In most cases, Zn(II) is coordinated by a combination of His, Glu/Asp, and Cys residues. Because Zn(II) is a borderline metal according to the hard-soft acid-base theory, it can coordinate well to both hard (nitrogen and oxygen) and soft (sulfur) donor atoms. Specifically, Zn(II) can coordinate to the N_δ or N_ε atom of the His ring, the $O_{\varepsilon 1}$ or $O_{\varepsilon 2}$ atom of Glu/Asp (*syn* or *anti*), or the S atom of Cys in either a monodentate or bridging fashion (Figure 1). More rarely, Zn(II) will also bind to the phenolate group of Tyr,[8] the carboxamide oxygen of Asn or Gln,[9,10] or a protein backbone carbonyl oxygen.[11] A detailed analysis of the amino acids coordinating zinc in proteins found in the Protein Data Bank (PDB) has been reported and is broken down by ligand as follows: His, 28%; Cys, 23%; Asp, 13%; Glu, 11%; other ligands (not amino acids), 9%; water, 15%; and other amino acids, 1% (of which the most significant are Ser, Thr, and Lys).[2]

There are several reasons for the prevalence of Zn(II) as a catalyst in enzymes. First, it is earth abundant, with concentrations of 30 ppb in seawater and 75 ppm in the earth's crust.[12] Compared to other first-row transition metals, Zn(II) stands out because its filled d orbital precludes it from participating in redox reactions and allows it to function solely as a Lewis acid. This particular property makes Zn(II) an ideal metal ion for reactions requiring a redox-stable cofactor to function as a Lewis acid catalyst. As a d^{10} metal ion, Zn(II) has zero ligand field stabilization energy, so no geometry is electronically more stable than another. This lack of an energetic barrier for Zn(II) may be important for its catalytic properties, allowing for changes in coordination number throughout the catalytic cycle (from four- to five-coordinate, for example, to accommodate the intermediate) and for alterations in the reactivity of the metal ion. Additionally, Zn(II) complexes can undergo rapid ligand exchange, enhancing the ability of Zn(II) to effect a catalytic cycle through efficient product release. Although no coordination number or geometry is inherently more stable, most zinc-

Received: December 14, 2013
Revised: January 23, 2014
Published: February 7, 2014

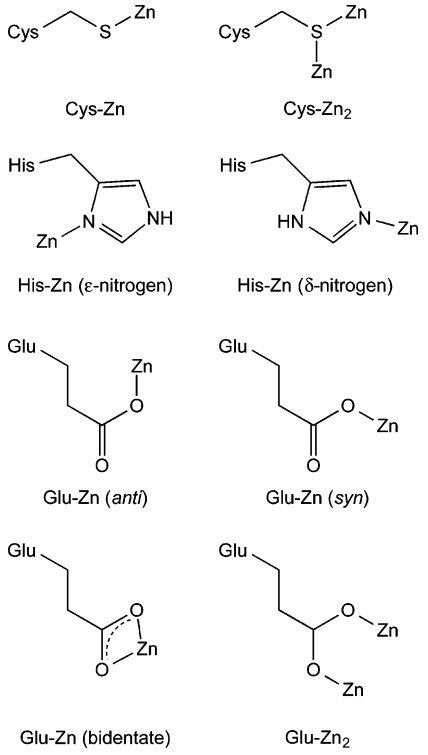

Figure 1. Zinc(II)−amino acid side chain binding modes as described in the text. Most zinc ligands in proteins are the side chains of cysteine (S donor), histidine (N donor), and glutamate or aspartate (O donor).

dependent proteins feature a resting state with a tetrahedral zinc center [in some cases, Zn(II) is found in a five-coordinate trigonal bipyramidal geometry].[2,13] This is in contrast to simple zinc complexes that have more instances of higher coordination numbers (e.g., 5 and 6).[14] Clearly, the protein plays a role in enforcing a lower coordination number. Zinc sites in proteins have been classified into three general categories: structural, catalytic, and cocatalytic.[6,15] Structural sites have a saturated coordination sphere with all metal ligands originating from amino acids and confer stabilization on the tertiary structure. On the other hand, catalytic sites require an open coordination sphere with at least one water molecule and three or four protein ligands and participate directly in the bond-making and bond-breaking process of a chemical reaction. Cocatalytic sites have several metals in proximity of each other, where one is directly catalytic and the others serve to enhance the activity. It is worth noting that while these basic guidelines for Zn(II) coordination are generally true, additional principles continue to emerge for Zn(II) sites at protein interfaces and inhibitor and transient binding sites in Zn(II)-transporting and Zn(II)-sensing proteins.[16,17]

Although Zn(II) is required for the function of enzymes in all six enzyme classes, the hydrolase class contains the most representatives (397 of a total of 933 zinc enzymes, including aminopeptidases, carboxypeptidases, matrix metalloproteinases, phosphatases, β-lactamase, etc.).[1,2] CA catalyzes the nucleophilic addition of OH^- to CO_2 and officially belongs to the lyase class of enzymes but will be discussed here in the context of hydrolytic enzymes. Notably, while CO_2 hydration is the physiological reaction for CA, this enzyme can also catalyze the hydrolysis of a number of other substrates, including the often-used and well-studied *p*-nitrophenyl acetate (*p*NPA).[18,19] The zinc hydrolase superfamily shares a common structural scaffold consisting of an eight-stranded β-sheet flanked by six α-helices. Although the active site is located at the end of the four central β-strands, in this class of zinc enzymes, there is little to no conservation between active site structure or amino acid composition.[20] Some members of this superfamily are monozinc enzymes (carboxypeptidase and thermolysin), while others contain cocatalytic zinc sites (aminopeptidase, β-lactamase, and alkaline phosphatase).[21] The binding residues around the catalytic Zn(II) ions follow the spacer rule, but their identities are not conserved.[7] The active sites can be comprised of differing residues, most commonly $His_2Glu/Asp(H_2O)$ (e.g., thermolysin and carboxypeptidase A)[22,23] and $His_3(H_2O)$ (e.g., CA),[24] but sometimes also $CysHis_2(H_2O)$ (e.g., bacteriophage T7 lysozyme),[25] $Cys_2His(H_2O)$ (e.g., liver alcohol dehydrogenase),[26] and even $Cys_3(H_2O)$ (e.g., 5-aminolevulinate dehydratase)[27,28] which can be located on a combination of loops, β-sheets, and α-helices.[2,13] One common feature is that the active sites are generally buried within the protein structure. There are multiple evolutionarily unrelated families for CA (α-, β-, γ-, δ-, and ζ-CAs),[29,30] although all are zinc enzymes. All 16 known isoforms of the most extensively studied α-family of CAs share a conserved monomeric tertiary structure mainly comprised of β-strands.[31] Specifically, the structure consists of 10 β-strands that form a large twisted β-structure surrounded by six α-helices on the surface of the molecule. The active site is located at the bottom of a cavity that reaches almost to the center of the molecule where Zn(II) is bound to three His residues and a solvent molecule in a tetrahedral geometry. The His residues are located along adjacent β-strands, two with a one-residue spacer between them on a single strand (His94 and His96) and the third separated by a longer spacer at position 119. These examples of zinc enzymes from the hydrolase and related lyase classes clearly illustrate variability in the coordination environment, yet most hydrolases are contained within a similar overall structure primarily comprising β-sheets where often at least one ligand originates from a loop region or the end of a secondary structural element. Numerous differences in protein structures encompassing hydrolytic zinc centers (some are small and monomeric, whereas others are complicated multimeric structures) may tune their interactions with substrates. Determining the patterns, if they exist, between the protein folds and functions for each zinc site is complicated at present, although important questions are the role of the protein fold in the metal center's activity and whether it is necessary or simply a remnant of evolution.

Along similar lines, while the variability that can be achieved through just four amino acids and their assorted binding modes is striking, it has been demonstrated that it is not simply the first coordination sphere that differentiates Zn(II) sites and functions from one another. Although the importance of secondary interactions is well-known,[17,32] reliable guidelines such as those for the first coordination sphere around Zn(II) are not yet well-defined. For example, not only is a $ZnHis_3$ site present in the metalloenzymes CA[33] and many matrix metalloproteinases (MMPs),[7] both where activation of a Zn(II)-bound water molecule to a hydroxide nucleophile occurs, it also exists as a structural anchor in insulin[34] (each His ligand originating from a different subunit) and as an inhibitor in serine protease tonin;[35] in ZnuA,[36] the $ZnHis_3$ site transports Zn(II) in the periplasm (Figure 2). This variability generates a number of questions. How can a single first coordination sphere be modified by the protein environment to result in such a wide variety of metalloprotein functions? What

dx.doi.org/10.1021/bi4016617 | *Biochemistry* 2014, 53, 957−978

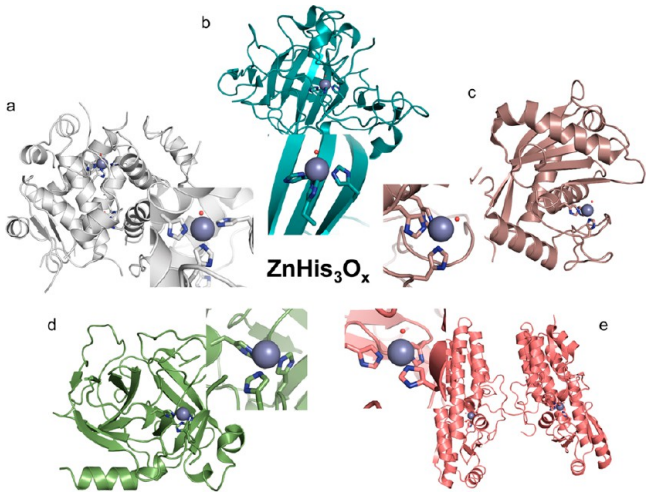

Figure 2. $ZnHis_3$ sites in various proteins.[16,17] (a) Insulin (PDB entry 1AIO), in which Zn(II) organizes the hexamer with His ligands originating from three different subunits.[34] (b) Carbonic anhydrase II (PDB entry 2CBA), in which Zn(II) forms a hydrolytic active site and each of the three His ligands is on a β-sheet.[33] (c) Matrix metalloproteinase adamalysin II (PDB entry 1AIG), in which Zn(II) forms a hydrolytic active site with two His ligands on an α-helix and the third from a loop.[193] (d) Serine protease tonin (PDB entry 1TON), in which Zn(II) binding inhibits activity.[35] (e) Zinc transporter ZnuA (PDB entry 1PQ4), in which the structure mediates Zn(II) mobility for transport.[36]

are the ligands and structures necessary for a given function? Is the native protein fold critical for optimal function? To what extent does the structure of the binding pocket discriminate different types of reactivity? Are there minimal changes that can be made around the metal site to alter or completely change the function? How many different functions can a single metal site perform? Although direct biochemical studies of existing metalloproteins have begun to answer some of these questions, it is difficult to imagine a situation in which a native enzyme can be mutated to determine the baseline requirements of the first coordination sphere in the absence of most of the surrounding protein matrix (the metal site would likely not fold and/or bind metal). Of course, this can be (and is often) approached by synthesizing small molecule models of the active sites of zinc metalloproteins, but this approach comes with a number of limitations, including difficulties in working under aqueous conditions, in using the natural amino acid ligands, in stabilizing lower coordination numbers within a hydrophobic core, and in assessing the influence of hydrogen bonding and electrostatics on catalytic activity.[37] Protein design is an effective yet challenging approach to re-creating functional metal sites found in native enzymes. With this process, one may replicate a proteinlike environment more straightforwardly than with synthetic models (using the real amino acid ligands, aqueous environment, etc.). The design itself can be approached in different ways.[38−48] One route is to redesign an existing native protein scaffold to incorporate a metal-binding site. Alternatively, one can design, de novo, both the protein scaffold and the metal-binding site. Successes seen with this approach are more rare; however, they may yield unprecedented information regarding hidden structural features.

Metalloprotein design studies collectively aim to illuminate the relationships between the metal site and surrounding protein structure and the corresponding function. Both rigorous de novo design and assorted redesign approaches can provide useful information to this end. Although this Current Topic will focus on the design of zinc metalloproteins, much of the information gleaned from these studies may be applied to the design of proteins coordinating a variety of different metals. The ultimate goal is to apply this work to the development of novel metalloproteins and enzymes for a variety of applications, which may be limited by only our understanding of how to design and prepare them.

■ ZN(II) AS AN ATTRACTIVE CATALYST IN PROTEINS

Zn(II) ions serve as powerful catalysts in many hydrolase enzymes with diverse, though generally related, mechanisms.[37,49,50] The reactivity of Zn(II) in enzymes centers around a Zn−OH_2 moiety (Figure 3). In the most common

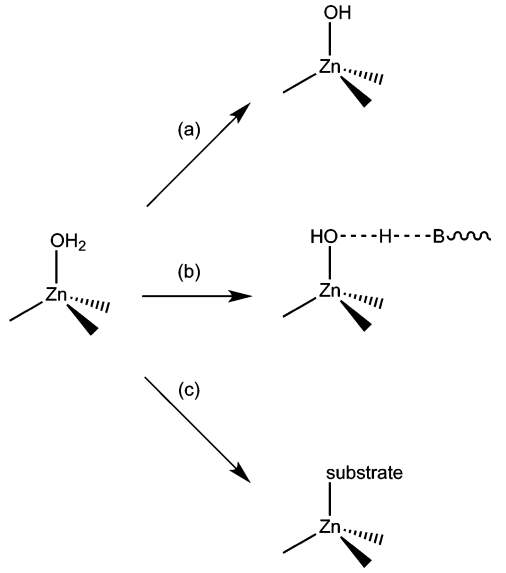

Figure 3. General mechanisms for mononuclear Zn(II) enzymes. (a) Ionization to form a Zn(II)−hydroxide nucleophile. (b) Polarization with the assistance of a general base to generate a nucleophile. (c) Displacement by the substrate that can be subsequently activated to generate a nucleophile.

mechanism, the Lewis acidic Zn(II) center simply promotes deprotonation of the coordinated water to generate a hydroxide species at neutral pH (as in the mechanism for CA[24,51,52]). For less Lewis acidic Zn(II) centers (such as that in carboxypeptidase, which has an anionic Glu residue in the coordination sphere[53]), further activation may occur by interaction with an adjacent base (such as a Glu residue) to generate the hydroxide species. A third type of mechanism involves displacement of the water molecule by substrate, which can then be activated (such as in 5-aminolevulinate dehydratase[54] or liver alcohol dehydrogenase[55]). There are also examples in which zinc can activate thiols toward nucleophilic attack, such as in the Ada DNA repair protein.[56,57] As will become apparent throughout the rest of this Current Topic, designed hydrolytic zinc proteins are generally intended to operate by the simple deprotonation mechanism and have not yet encompassed the design of nearby basic residues to assist in deprotonation (a feature of many of zinc hydrolases), nor have they been tested for activation of substrates such as alcohols.

dx.doi.org/10.1021/bi4016617 | *Biochemistry* 2014, 53, 957−978

DESIGNING ZINC-BINDING PROTEINS

De Novo Sites in de Novo and Preexisting Scaffolds.

Given the importance of zinc, it is not surprising that zinc site design was among the initial metalloprotein design reports. In the earliest work, $ZnHis_3$ sites (as inspired by CA) were engineered into the de novo-designed four-helix bundle protein, α4,[58] and the redesigned antibody-like protein, minibody.[59] In the case of α4, the binding of Zn(II) to the His_3 site helped to decrease the protein's molten globule-like properties (because of a lack of conformational specificity in the core) and induce a more nativelike protein fold, although no structure or binding affinity was reported.[60] In the minibody reported by Pessi et al., a 61-residue all β-sheet structure, the dissociation constant for Zn(II) binding was estimated to have a lower limit of $\sim 10^{-6}$ M (Figure 4a).[59] While this represents fairly strong binding, it is relatively weak when compared to that of native zinc enzymes that generally have dissociation constants in the nanomolar to picomolar range.[61−64] A Zn(II)-binding His_3 site was also introduced into the retinol binding protein in a solvent-exposed position on the surface.[65] The dissociation constant for binding of Zn(II) to this site is stronger and closer to the range for native zinc proteins (36 ± 10 nM). The geometry, based on competition with chelating ligands, is likely octahedral, with three open coordination sites.[66] Soon after, a scorpion toxin, charybdotoxin (37 amino acids and comprised of a short α-helix on one face and an antiparallel triple-stranded β-sheet on the opposite with three stabilizing disulfide bonds in the interior), was used as a small scaffold for the incorporation of a His_3 site (Figure 4b).[67] Nine mutations were made to incorporate the metal-binding site, including engineering in three His sites and including the Gln and Glu residues found in CA that form hydrogen bonds to two of the primary His residues. While X-ray crystal or NMR structures were not reported, CD and ^{1}H NMR indicate that the structure is largely retained relative to the parent sequence. The dissociation constant for Zn(II) binding is $(5.3 \pm 0.4) \times 10^{-6}$ M, and although no catalytic activity was reported, the design demonstrates the achievement of a stable, yet solvent-exposed metal-binding site at the surface of a miniprotein.[63,68] Table 1 summarizes the known dissociation constants for many of the designed Zn(II)-binding sites that are reported. It should be noted that these metal binding affinities are determined using various methods [e.g., isothermal titration calorimetry (ITC), equilibrium dialysis, and absorbance or fluorescence spectroscopy] under various conditions, some which are thermodynamic and others of which are based on metal site activity. As such, these metal site affinities should be relied

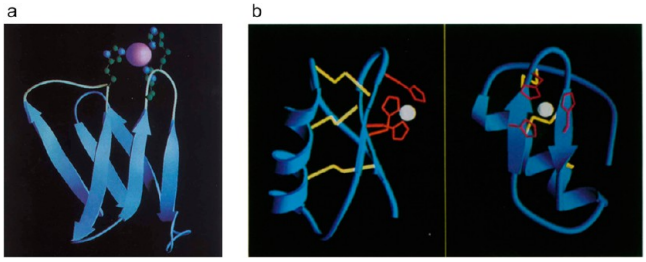

Figure 4. (a) Modeled structure for the design of the minibody and its predicted metal-binding site (His_3). Panel a was reprinted from ref 59. Copyright 1993 Nature Publishing Group. (b) Model of the redesigned scorpion toxin charybdotoxin (orthogonal views) with a His_3 metal-binding site. Disulfide bonds are colored yellow. Metal-binding ligands are colored red. Panel b was reproduced from ref 67. Copyright 1995 National Academy of Sciences.

Table 1. Comparison of Zn(II) Binding Affinities for Selected Designed Proteins

design	coordination site	K_d(Zn(II)) (M)	pH	ref
minibody	His_3	$\sim 10^{-6}$	not available	*a*
retinol binding protein	His_3	$(3.6 \pm 1.0) \times 10^{-8}$	not available	*b*
charybdotoxin	His_3	$(5.4 \pm 0.4) \times 10^{-6}$	6.5	*c*
IZ-3aH	His_3	9×10^{-6}	7.0	*d*
IZ-3adH	His_6	$(2.3 \pm 0.2) \times 10^{-5}$	7.0	*e*
Zα4	His_2Cys_2	2.5×10^{-8}	7.5	*f*
Zβ1M,A,L	His_3Cys	$\sim 1 \times 10^{-9}$	7.5	*g*
Trx[ZS].C and Trx[ZS].F	His_2Cys_2	$\sim 1 \times 10^{-8}$	7.5	*h*
Trx[ZS].A, Trx[ZS].B, and Trx[ZS].E	His_2Cys_2	$\sim 1 \times 10^{-6}$	7.5	*h*
BABZ5	His_2Cys_2	2.2×10^{-6}	7.3	*i*
IGA	Cys_4	4×10^{-16}	8.0	*j*
		4×10^{-12}	7.0	*j*
GGG	Cys_4	1.8×10^{-17}	pH-independent	*k*
		5×10^{-13}	7.4	*k*
	$HisCys_3$	7×10^{-16}	pH-independent	*k*
		5×10^{-13}	7.4	*k*
	His_2Cys_2	4×10^{-14}	pH-independent	*k*
		5×10^{-13}	7.4	*k*
$\alpha\beta\beta$ Zn(II)-hydrolase	His_3	8×10^{-4}	not available	*l*
$[Zn(II)(H_2O/OH^-)]_N$ (**TRI**L2WL23H)$_3^{n+}$	His_3	$(0.6 \pm 0.1) \times 10^{-6}$	7.5	*m*
$[Hg(II)]_S[Zn(II)(H_2O/OH^-)]_N$ (**TRI**L9CL23H)$_3^{n+}$	His_3	$(0.8 \pm 0.1) \times 10^{-6}$	7.5	*m*
$[Zn(II)(H_2O/OH^-)]_N[Hg(II)]_S$ (**TRI**L9HL23C)$_3^{n+}$	His_3	$\sim 8 \times 10^{-6}$	7.5	*m*
$[Hg(II)]_S[Zn(II)(H_2O/OH^-)]_N$ (**TRI**L9CL19H)$_3^{n+}$	His_3	$(3.7 \pm 1.3) \times 10^{-6}$	7.5	*m*

[a]From ref 59. [b]From ref 65. [c]From ref 67. [d]From ref 82. [e]From ref 83. [f]From ref 69. [g]From ref 76. [h]From ref 84. [i]From ref 85. [j]From ref 87. [k]From ref 75. [l]From ref 151. [m]From ref 168.

dx.doi.org/10.1021/bi4016617 | *Biochemistry* 2014, 53, 957−978

upon only as a broad, general comparison between different sites.

The de novo-designed four-helix bundle, α4, was also used as a scaffold for the incorporation of a closed-sphere $ZnCys_2His_2$ site (Zα4), much like the structural site found in zinc finger (ZF) proteins (Figure 5a).[69,70] Co(II) was used as a spectroscopic probe to demonstrate successful design of a tetrahedral site. It should be noted that recent literature indicates that although Co(II) substitution in Zn(II) enzymes may result in the same coordination environment, there are a number of cases in which an identical coordination environment does not result.[71] Mutants of this design, in which one ligand was removed at a time (by substitution with Ala) to generate an open coordination site, were also tetrahedral, although the Co(II) binding affinities were all decreased by at least 1 order of magnitude. Overall, the Cys residues were thought to be stronger determinants for Co(II) binding than His, which is not unexpected because the negative charge on the Cys thiolate residue is known to provide a stronger binding contribution.[72−75] Klemba et al. reported the redesign of the B1 domain of IgG-binding protein G (a 56-residue protein with a four-stranded β-sheet crossed by a single α-helix) to incorporate a closed-sphere His_3Cys site for binding Zn(II) (Figure 5b).[76] Co(II) confirmed the presence of a tetrahedral site, and on the basis of the competition, the dissociation constant for Zn(II) binding was estimated to be on the order of 10^{-9} M. There are also numerous other studies involving the design of a variety of peptide ligands for the preparation of metal sites meant to mimic ZF proteins [coordination environment $Zn(Cys)_{4-x}(His)_x$, where x = 0, 1, or 2], which are beyond the scope of this Current Topic.[77,78] Overall, these examples of designed Zn(II) sites with four protein ligands generally display higher affinities than the designed sites with three protein ligands discussed above. It is worth noting that no strict correlation exists between the number of ligands bound in the first coordination sphere for native zinc enzymes and their Zn(II) binding affinities.[16,61,64] This is likely due to the incorporation of secondary interactions and demonstrates the utility of protein design to uncover features of metal binding that would otherwise be difficult to determine in a native system.

Recently, the Baker group designed a high-affinity Zn(II)-binding site using a computational design approach to incorporate the unnatural amino acid (2,2′-bipyridin-5yl)-alanine (Bpy-Ala).[79] Using RosettaMatch to identify appropriate backbone geometries and a negative design approach to disfavor undesirable coordination environments, the group engineered an octahedral metal-binding site comprised of Bpy-Ala, Asp, Glu, and two water molecules. Although the site binds a number of divalent metal cations, including Co(II), Fe(II), and Ni(II), competition experiments estimate that the metal binding affinity of Zn(II) is ∼40 pM. The preorientation of the two metal-binding pyridine nitrogen atoms from Bpy-Ala likely contributes to this high metal binding affinity by lowering the entropic cost of orienting ligands (e.g., His) for metal binding, therefore demonstrating the power of using nonnatural amino acids for designing metal-binding sites.

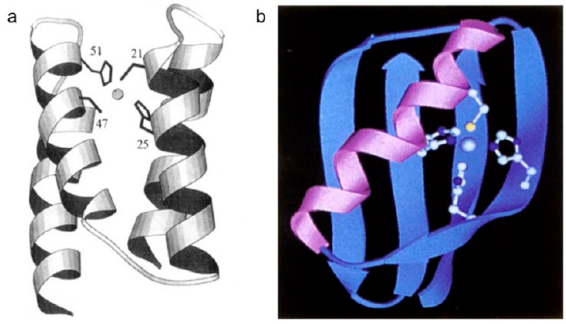

Figure 5. (a) Model of Zα4. The side chains (clockwise from top right) are Cys21, His25, Cys47, and His51. Panel a was reproduced from ref 70. Copyright 1995 American Chemical Society. (b) Model of the metal-binding site in the B1 domain of streptococcal protein G. The ribbon diagram is specifically of Zβ1M. The side chains around the metal-binding site are His16, His18, His30, and Cys33. Panel b was reproduced from ref 76. Copyright 1995 Nature Publishing Group.

Metal-Mediated Stabilization of Protein Structures. There are a number of examples in which designed Zn(II)-binding sites have resulted in enhanced folding of partially or completely unfolded peptide structures.[75,80−87] A His_3 site was introduced into a de novo-designed three-stranded coiled coil (3SCC), IZ [$YGG(IEKKIEA)_4$], to generate IZ-3aH, which folds in the presence of Zn(II) (K_d = 9 μM), although no X-ray crystal structure was reported.[82] The same group reported a similar 3SCC, but with six His residues available for binding in an octahedral geometry with a K_d for Zn(II) binding of 23 ± 2 μM.[83] These affinities remain in the same range as those described above for Zn(II) sites with three protein ligands (Table 1).

Wisz et al. reported the semiautomated design of a series of $ZnCys_2His_2$ centers into the non-metalloprotein thioredoxin (Trx, using Dezymer[88]) (Figure 6).[84] Dezymer was used to identify sites where appropriate amino acids could be engineered to create a metal-binding site with predetermined geometry, in this case tetrahedral. Visual inspection identified seven variants with buried potential metal sites and few steric clashes with the backbone. Five of seven experimentally characterized mutants bound Co(II) in a tetrahedral geometry with strong dissociation constants for some (2−4 μM) and weak for others (150−250 μM). Zn(II) binding (measured by displacement) was 2−3 orders of magnitude stronger than Co(II) binding (nanomolar to micromolar K_d). The strongest dissociation constants were for structures in which the apo form

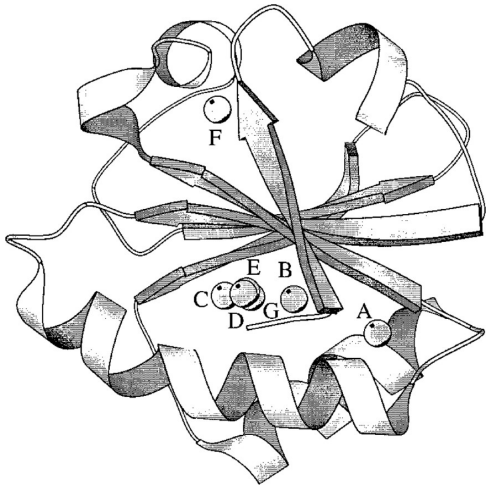

Figure 6. Distribution of the designed Cys_2His_2 sites in thioredoxin (letters identify each design). This figure was reproduced ref 84. Copyright 1998 American Chemical Society.

dx.doi.org/10.1021/bi4016617 | Biochemistry 2014, 53, 957−978

was stable and metal binding further increased the stability (Trx[ZS].C and Trx[ZS].F). In two cases (Trx[ZS].A and Trx[ZS].B), the apo form was unstable and metal binding induced folding [Co(II) K_d values of ~150 μM]. In the fifth case (Trx[ZS].E), the apo form was stable but metal binding decreased the stability. The weak metal binding affinity for this variant results from clashing steric interactions within the metal coordination sphere. Thermodynamic analysis revealed that all variants bound metal to the unfolded state, and the observed metal-mediated stability is a consequence of differential binding to the folded native state and unfolded structures, although the dominant factor for binding to the unfolded state is unclear. This work demonstrates how the design of a family of similar sites within the same scaffold can lead to an understanding of how both the intrinsic properties of the metal center and the surrounding protein matrix can affect the metal binding affinity (and stabilization). In this case, the metal dictates geometry and the thermodynamic price paid by the protein to accommodate the metal is reflected in the binding constant. Important considerations for designing metal-binding sites are that packing interactions in the binding site should be carefully considered to avoid costly reorganization energies and binding to the unfolded stable should be destabilized (negative design).

Another example examining the design of a $ZnHis_2Cys_2$ site in several locations of a protein (de novo-designed DS119 with $\beta\alpha\beta$ structure) was reported by Zhu et al.[85] It was found that Zn(II) sites designed into the protein core generally destroyed the folding even in the presence of zinc, while those at flexible terminals or loops displayed Zn(II)-induced aggregation, with dissociation constants in the range of 2−20 μM; however, the binding stoichiometry was 1:1 in only one case [BABZ5 (K_d = 2.2 μM)]. These observations result from a balance between the energy provided by metal binding and the cost of folding the protein. In the cases where the engineered ligands destroy the core of the protein, energetic contributions from the binding of Zn(II) are not enough to recover the fold.

Overall, these design studies in which metal binding induces or further stabilizes a protein fold demonstrate a connection between the binding constant and the energy required to fold a given protein. The formation of metal−ligand bonds provides a favorable enthalpic contribution to the free energy of protein folding. There are also entropic contributions from the release of water molecules from the binding site and the solvated metal upon binding. In an effort to separate protein−protein and metal−protein contributions to the free energy of folding, Reddi et al. reported the thermodynamic analysis of binding of Zn(II) to a Cys_4 site in a minimal, unstructured, 16-mer peptide, **GGG** (a variant of **IGA** with the sequence NH_2-KLCEGG·C*GG*CGGC·GGW-$CONH_2$).[86] Petros et al. had initially reported the design of a structural ZnS_4-binding site in a de novo-designed 16-amino acid peptide ligand, **IGA** (sequence H_2N-KLCEGG-CIGCGAC-GGW-$CONH_2$),[87] and found apparent dissociation constants for Zn(II) at pH 8.0 of 0.4 fM and at pH 7.0 of 4 pM [similar to that for a redesigned ZF, CP1-CCCC (K_d = 1.1 pM[89])]. These are well within the range observed for natural zinc proteins like metallothionein (K_d = 0.1 pM at pH 7.0),[64] yet (at pH 7.0) weaker than those of the zinc sensor proteins ZntR and Zur (K_d = 1.5 and 1.1 fM, respectively).[61,90] It was suggested from this work that the formation of the $ZnCys_4$ site provides a −22.1 kcal mol^{-1} driving force for protein folding. The goal of the work using **GGG** [designed to more closely resemble structural Zn(II) sites than **IGA**, which was originally based on a [4Fe-4S] binding motif] was to decouple the metal binding and protein folding events by choosing a structure in which the free energies of the folded and unfolded states are identical. The results indicate that Zn(II) binding is entropy-driven and controlled by proton release. The pH-independent dissociation constant for binding of Zn(II) to **GGG** is 18 × 10^{-18} M (18 aM), indicating that a $ZnCys_4$ site can provide up to −22.8 kcal mol^{-1} of driving force for protein structure stabilization (Figure 7).[75] The majority of the driving force is due to dehydration of the metal and binding site, so the process is largely entropy-driven. $ZnCys_3His$ and $ZnCys_2His_2$ sites were also examined with similar results and dissociation constants of 0.7 fM (and a −20.7 kcal mol^{-1} contribution to protein stability) and 40 fM (a −18.3 kcal mol^{-1} contribution), respectively. The observation that the Cys thiolate is a better ligand for Zn(II) than His is again consistent with literature precedent.[72−75] However, it should be noted that at physiological pH (7.4), the contributions from each of the differing coordination motifs are equal, because of proton competition with the Cys ligands, given that the thiols (in the apo peptides) have pK_a values in the range of 7.8−9.1. The dissociation constant for binding of Zn(II) to each peptide (Cys_4, Cys_3His, and Cys_2His_2 sites) is the same, 0.5 pM, with the same −16.8 kcal mol^{-1} energetic contribution to the protein folding driving force from metal binding. This driving force results from a combination of the favorable entropic contribution from proton loss and the unfavorable enthalpic contribution from thiol deprotonation. In natural proteins, which can have weaker binding affinities for the same coordination motifs, the difference may be due to the loss of Zn(II) binding energy to protein folding. We also note that the role of the binding pocket itself is important and can affect the energy needed for metal binding.

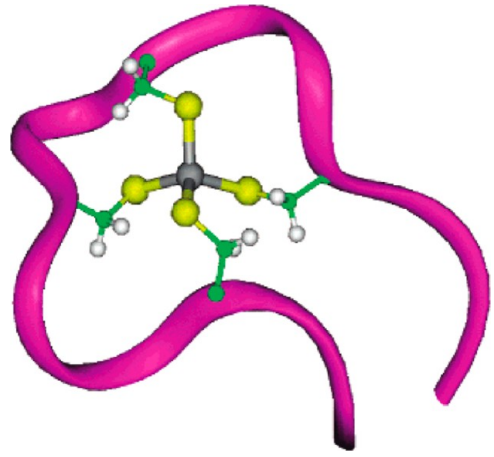

Figure 7. Molecular model of the Zn(II)−**GGG** complex with a Cys_4 site rendered using Biosystem Insight II. This figure was reproduced from ref 86. Copyright 2007 American Chemical Society.

The work described in this section, although focused on structural zinc sites, is important in the context of this Current Topic because it highlights several aspects of metal binding and protein folding that must be considered when designing zinc metalloenzymes. The energetic cost of protein folding should be minimized in both the apo form and the metal-bound form to minimize the reorganization requirements upon metal binding. Next, the binding of metal should be optimized toward the folded state rather than the unfolded state while keeping the structure flexible enough to allow for metal and

substrate binding. Although very high binding affinities may be achieved for unfolded structures such as designed peptides **IGA** and **GGG** and natural ZFs, catalytic zinc sites will likely require further structural contributions from a larger protein matrix for the stabilization of unsaturated coordination spheres and substrate binding. Additionally, although Cys residues can clearly provide more favorable Zn(II)−ligand interactions, their effects on the Lewis acidity of the Zn(II) center must be considered and will be discussed below. Therefore, designing catalytic zinc sites will require striking a balance between achieving sufficiently strong Zn(II) binding to promote catalysis [the affinities reached using **IGA** and **GGG** variants are certainly higher than those observed for effective native Zn(II) enzymes] and forming well-folded protein structures.

Metal-Mediated Stabilization toward the Preparation of Designed Multimeric Structures. Another approach for the design of structural metal sites (and, in some cases, catalytic sites) in proteins that is gaining ground in recent years is to use the binding energy provided by metals to direct the folding and assembly of multiple protein subunits and even extended nanostructures. Although metalloprotein design is typically associated with incorporating stable metal sites into protein cores, metal−protein surface interactions are at least equally significant, and metal sites are often located at the interfaces of multimeric protein complexes. Additionally, the formation of metal sites at protein interfaces has been proposed as a possible evolutionary route toward efficient metalloenzymes. Therefore, gaining a full understanding of how this might occur through a design approach should prove to be very important. This topic has been reviewed,[91−93] but the strategy has since expanded to include the generation of periodic protein arrays[94] and, as will be discussed below, the design of a hydrolytic zinc metalloenzyme.[95,96] Briefly, the Tezcan group has focused on using metal-coordinating motifs on the surface of a monomeric protein, cytochrome cb_{562}, to engineer novel protein−protein interaction interfaces to control the assembly of proteins. The initial model system, MBPC-1 (metal binding protein complex), has two bis-His motifs on its surface which, upon addition of equimolar amounts of divalent metals [Zn(II), Cu(II), and Ni(II)], forms discrete multimeric structures according to the stereochemical preferences of the metal ions.[91,97,98] Subsequent computational redesign using Rosetta-Design[99] optimized the hydrophobic packing between interfaces and included additional hydrogen bonding and salt bridge interactions to convert the Zn(II)-mediated tetramer into a structure that could self-assemble even in the absence of metals.[100] The Tezcan group also successfully incorporated nonnatural metal chelates onto the surfaces to generate not only coordinatively unsaturated metal sites but also a site that enforces a nonpreferred geometry on a metal due to the steric bulk of the chelates (a buried conformation is 4.2 ± 1.3 kcal mol^{-1} more favorable than an extended conformation for Phen, or 1,10′-phenanthroline, in MBPPhen2) and lattice packing arrangements that hold the metal centers in proximity of each other (Figure 8).[101] This is of particular importance to the design community because an efficient metalloenzyme often requires coordinatively unsaturated metal sites with strained metal geometries. More recently, the group also reported the design of a self-assembling Zn(II)-binding protein cryptand, in which a $ZnHis_3(H_2O)$ site is achieved in a structure templated by disulfide bonds. Although Zn(II) binds well (four total sites in a tetrameric structure, where $K_{d,4Zn}$ = 480 ± 35 nM), no esterase activity was observed (toward *p*NPA), possibly because

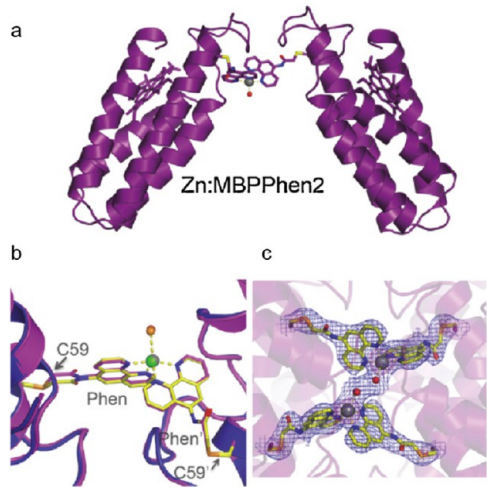

Figure 8. (a) Crystal structure of the Zn−MBPPhen2 dimer (PDB entry 3MNK).[101] (b) Superposition of Ni−MBPPhen2 (yellow) and Zn−MBPPhen2 (magenta) metal centers. (c) Close-up showing the proximity between the coordinatively unsaturated metal centers in the asymmetric unit of the Zn−$MBPPhen2_2$ structure. The $2F_o - F_c$ electronic density map is contoured at 1.2σ. The dimer is formed in solution and in the solid state. This figure was reproduced from ref 92. Copyright 2011 Elsevier.

the Zn(II) sites are not very accessible (Figure 9).[102] While assembly processes can lead to structures under kinetic control, achieving these unsaturated metal sites with designed proteins requires structures that strike the delicate balance between thermodynamic stability at the metal site and over the whole peptidic structure.

Reengineering Preexisting Metal Sites for Hydrolytic Activity. Beyond the introduction of Zn(II)-binding sites into both de novo and existing protein scaffolds through the variety of approaches discussed above, existing Zn(II) sites can be redesigned to introduce new functions or alter existing functions. In this section, we will first describe extensive mutagenesis studies on CA, which is a desirable target for many protein design studies. Then we will discuss a design study involving the related MMPs, which, like CA, have a $ZnHis_3(H_2O)$ active center.[103] We will then discuss the more extensive redesign approach of an enzyme, glyoxolase II, structurally unrelated to CA and MMP but that still performs hydrolytic catalysis.[104] Finally, we will discuss the redesign of native zinc proteins, which are not initially catalytic but have mononuclear structural zinc sites.[105,106] Additionally (although we will not go into further detail here), there are several examples of using Zn(II)-binding sites to control or alter different protein functions. These studies range from the design of Zn(II)-binding sites for inhibition[107,108] or control of specificity of protease activity in trypsin[109−111] to Zn(II)-induced conformational changes for sensing[112−114] and control of various protein functions.[115,116]

Although there are many examples of zinc metalloenzymes that have been studied through alteration of their zinc coordination spheres, none have been more extensively reengineered than CA. This enzyme represents a target for achieving efficient hydrolytic catalysis for many designed zinc metalloproteins, so here we will summarize selected reengineering studies for CA (Figure 10). The direct metal-binding residues around the Zn(II) site (His94, His96, and His119) have been replaced by a variety of amino acids (Asp, Glu, Asn,

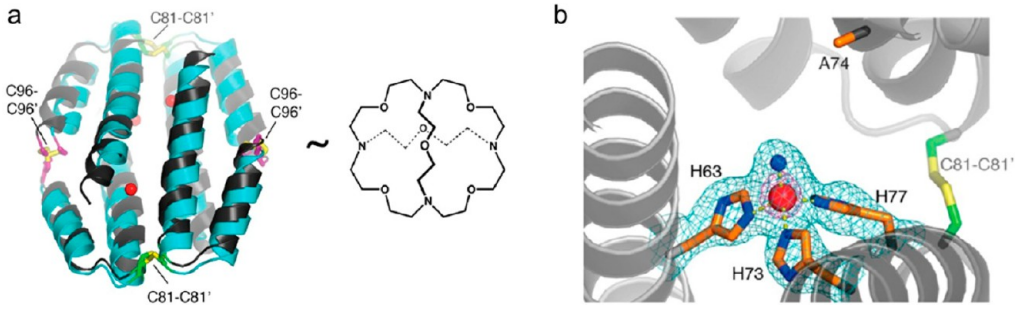

Figure 9. Overall structure and example of a Zn(II) site in a self-assembling protein cryptand templated by disulfide bonds. (a) Overlay of protein backbones of the apo and Zn(II)-bound forms of $^{C81/C96}RIDCl_4$. (b) One of four $ZnHis_3(H_2O)$ sites in $^{A74/C81/C96}RIDCl_4$ with the $2F_o - F_c$ electron density map contoured at 1.4σ (cyan) and 7σ (magenta). This figure was reproduced from ref 102. Copyright 2013 American Chemical Society.

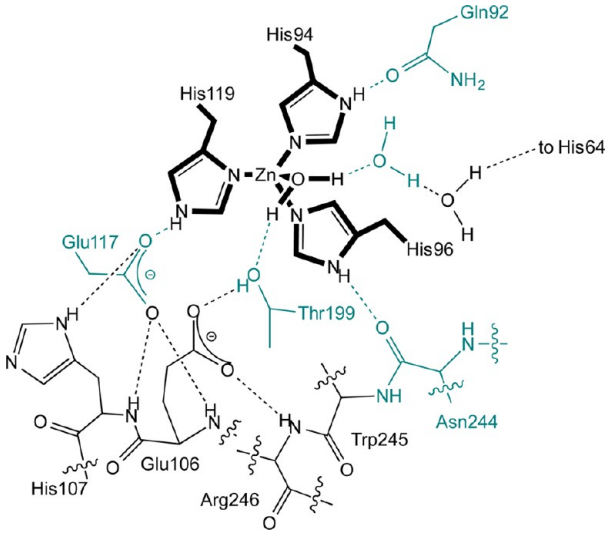

Figure 10. Schematic of the active site structure of carbonic anhydrase II displaying the extended active site around the Zn(II) center.

Gln, Cys, and Ala) to study the effects on the first coordination sphere.[24,117] Early work involved the preparation of the H94D mutant, which resulted in a tetrahedral His_2Asp coordination environment with a solvent molecule.[118] An ~10^4-fold loss of metal binding affinity was observed [K_d = 15 nM (Table 2)],

Table 2. Coordination Environments and *p*NPA Hydrolysis Rate Constants of Zinc Finger Mutant Peptides[a]

ZF variant	coordination no. (no. of vacant sites)[b]	*p*NPA hydrolysis rate constant (M^{-1} s^{-1})
Zn(II)−zf(CCHH)	4 (0)	0
Zn(II)−zf(CCGH)	5 (2)	0.218 ± 0.0085
Zn(II)−zf(CCAH)	5 (2)	0.232 ± 0.0051
Zn(II)−zf(CCHG)	5 (2)	0.351 ± 0.0182
Zn(II)−zf(CCHA)	4 (1)	0.568 ± 0.0228
Zn(II)−zf(GCHH)	5 (2)	0.399 ± 0.0014
Zn(II)−zf(CGHH)	5 (2)	0.458 ± 0.0021
Zn(II)−zf(AHHH)	6 (3)	0.478 ± 0.0057
Zn(II)−zf(HAHH)	6 (3)	0.497 ± 0.00058
Zn(II)−zf(HHAH)	6 (3)	0.370 ± 0.0289
Zn(II)−zf(HHHA)	6 (3)	0.443 ± 0.0147
Zn(II)−zf(HHHH)	6 (2)	0.966 ± 0.0492

[a]Taken from ref 105. In 20 mM HEPES buffer (pH 7.5), 0.1 M NaCl, and 3.5% acetonitrile at 25 °C. [b]Based on Co(II)-substituted UV−vis absorption studies.

probably in part due to the movement of the Zn(II) ion ~1 Å toward the Asp residue, resulting in the interruption of the evolved His_3 ligand arrangement. Although a recent report using ITC demonstrated a weaker Zn(II) binding affinity (K_d = 0.5 nM)[119] for CA compared to that previously reported (K_d = 0.8 pM),[120] we will continue to refer to previous values for consistency between mutants. Changes in the electrostatics of the site (neutral to anionic substitution) also lead to an increase in the pK_a for Zn-OH_2 deprotonation (as in Figure 3a) from 6.8 to >9.6. A larger loss of Zn(II) binding affinity is observed when His94 is replaced with Ala (K_d = 270 nM).[117] Substitution of the same His residue with a Cys also results in an ~10^4-fold loss of Zn(II) binding affinity [movement of the Zn(II) ion toward Cys is essentially the same as that observed for Asp in H94D] and an increase in the pK_a to >9.5.[117,121] Acknowledging that Cys substitutions in the designed structures discussed earlier led to increased binding affinities, we find it is worth noting that the apparent discrepancy described here is likely the result of interrupting the binding site structure of a highly evolved protein. Overall, changes to the charge of the zinc site by addition of charged residues result in severe losses to catalytic activity [altered Lewis acidity of Zn(II)]. However, when alternate neutral residues (Asn and Gln) are introduced, reasonable catalytic activity is retained, although ~10^4−10^5-fold losses of binding affinity are still observed.[10] Altering the other His positions in similar ways gives similar results.[117,122] Interestingly, a route toward improving the affinity of Zn(II) for CA has also been taken by substituting a nearby residue [Thr199, which forms a stabilizing hydrogen bond with the Zn(II)-bound solvent] with Cys, Asp, Glu, or His. Substitution with Cys results in an improvement in the K_d (from 4 to 1.1 pM) and some loss of activity (~10^3-fold) due to an alternate conformer with a Zn(II)−hydroxide species.[62,123] In the case of T199E, the affinity is greatly improved (K_d = 20 fM) and the activity is abolished because of the displacement of Zn(II)-bound hydroxide.[124] For T199H, the affinity actually decreases 20-fold as the fourth His does not bind to Zn(II).[124] Another example that alters the secondary coordination sphere is the mutation of Thr199 to Ala (abolishing the hydrogen bond), which retains the His_3 coordination environment, but results in a 100-fold loss of activity and an increase in the pK_a of ~1.5 units. Further, Glu106 forms a hydrogen bond acceptor interaction with Thr199, resulting in a zinc−hydroxide−threonine−glutamate hydrogen-bonding network. When Glu106 is substituted with Ala or Gln, to abolish this "secondary" hydrogen bond, the catalytic efficiency for CO_2 hydration is diminished ~10-fold to 9.5 or 23 μM^{-1} s^{-1},

dx.doi.org/10.1021/bi4016617 | *Biochemistry* 2014, 53, 957−978

respectively (although the k_{cat} values are ~1000-fold slower, suggesting a stronger effect on HCO_3^- dissociation and/or proton transfer steps than on the CO_2−HCO_3^- interconversion rates at the metal center), and that for *p*NPA hydrolysis is nearly 100-fold less efficient (30 and 40 M^{-1} s^{-1} for E106A and E106Q, respectively).[125] The pK_a for the E106A mutant increases to 7.9, while that for E160Q (pK_a = 7.1) is similar to that of wild-type CAII (pK_a = 6.8). There are also hydrogen bonding interactions with unbound nitrogen atoms of each of the His residues in the primary coordination sphere (His94 to Gln92, His119 to Glu117, and His96 to the backbone of Asn244). The effects of mutating Gln92 and Glu117 on the pK_a are within ±1 unit with only subtle effects on the K_d and losses of activity of ~10-fold or less. This is likely because the direct metal ligands will often replace the lost hydrogen-bonding partners with other protein sites or even solvent.[126−128] One case in which drastic effects were observed is that of the E117Q mutant, in which a 55000-fold loss of activity, an increase in the pK_a to >9, and a 1100-fold weaker Zn(II) binding affinity were reported.[129] These results have been proposed to arise from reversal of the hydrogen bond between residue 117 and His119, stabilizing His119 as a histidinate anion.

These studies on the primary and secondary coordination spheres of CA clearly demonstrate many of the characteristics of successful Zn(II) sites that should be taken into account in the protein design approach. Specifically, mutagenesis studies demonstrate that neutral His ligands in the primary coordination sphere are essential for enhancing the net positive charge at the Zn(II) site. Anionic protein ligands lead to a decrease in the Lewis acidity of Zn(II) with an increase in the Zn(II)−OH_2 pK_a. Substitutions in which the primary coordination sphere was altered but maintained at three protein ligands resulted in a loss of binding affinity, regardless of the charge of the ligand. This is contrary to the studies described above for designed peptides and proteins, in which thiolate ligands result in stronger binding affinities for Zn(II) than His ligands, therefore highlighting both the importance of the evolved metal site structure in a native protein and the difficulty in examining separate factors for metal site structure using a native metalloprotein. Of course, an open coordination site is required for catalysis, and hydrogen bonding interactions, such as those involving the primary His ligands and Zn(II)-bound solvent, can fine-tune Zn(II) binding affinities and pK_a values. Loss of these interactions typically results in a decreased binding affinity, a decreased activity, and an increased pK_a.

There are also several reports on the redesign of carbonic anhydrase for improved activity toward alternate ester substrates, in which controlling the steric interactions within the hydrophobic pocket can lead to altered substrate specificities and esterase activities.[19,130−132] Therefore, protein design efforts should also consider how size and charge interactions of the desired substrates could affect activity and control selectivity.

An alternative approach to enzyme mutagenesis studies is to retain the enzyme active site sequence while removing the remainder of the structure. A related class of enzymes, which also contain a catalytic zinc site comprised of three His residues and a solvent molecule, are the MMPs.[133] MMPs are the main processors of extracellular matrix components and perform hydrolytic cleavage of amide bonds. The catalytic domain contains a well-conserved sequence, including the His triad and also a nearby Glu residue that is crucial for catalysis (HExxHxxGxxH). A recent report analyzed a peptide corresponding to the Zn(II)-binding sequence from human MMP13 (Ac-KAHEFGHSLGLDHSK-NH_2) to determine its suitability as a flexible and minimal chemical model for the more rigid metal-binding sites found in native metalloproteins.[103] Potentiometric, CD, NMR, and mass spectrometric techniques support Zn(II) binding in a $His_3(H_2O)$ environment at pH 7 with a pK_a of 7.59 for deprotonation of Zn(II)−OH_2. Formation of a dihydroxide Zn(II)−$(OH^-)_2$ species occurs with a pK_a of 8.60. Given the similarity of these coordination environments to those of native zinc metalloenzymes such as the MMPs and CA, the Zn(II)−peptide complexes were tested for their ability to catalyze *p*NPA hydrolysis. The second-order rate constants are 0.24 and 1.44 M^{-1} s^{-1} for the mono- and dihydroxide species, respectively (these rate constants were determined by fitting observed rates between pH 7.4 and 9.2 to the equation $k_{obs,corr} = k_{ZnHL}[ZnHL] + k_{ZnL}[ZnL]$, where ZnHL is the monohydroxide species and ZnL is the dihydroxide complex). At pH 8.7, the initial rates were measured as a function of substrate concentration for the dihydroxide species and yield a catalytic efficiency of ~1.2 M^{-1} s^{-1}. While this activity compares favorably with those of small molecule models with similar structures,[134−136] it further highlights the importance of a preorganized protein structure for acquiring native enzymelike activity.

Another example of reengineering a zinc metalloenzyme is the computational redesign of the dizinc-containing glyoxalase II enzyme into a β-lactamase.[104] Both of these enzymes have reactions somewhat different and structures (dizinc metal sites) very different from those of the two zinc enzymes discussed above. Glyoxalase II catalyzes the hydrolysis of the thioester bond of *S*-D-lactoylglutathione, an important step in the conversion of toxic 2-oxoaldehydes into their corresponding 2-hydroxycarboxylic acids.[137] The active site structure includes two Zn(II) centers bridged by a water molecule and an Asp residue. One of the Zn(II) ions is further coordinated by three His residues and the other by one Asp and two His residues. The dizinc site found in metallo-β-lactamases, which catalyze the hydrolysis of β-lactam amide bonds to inactivate β-lactam antibiotics, is similar. However, the Zn(II) centers are linked by a hydroxide molecule; one Zn(II) ion remains coordinated to three His residues, and the other is coordinated to Asp, Cys, and His residues in *Bacteroides fragilis* and *Bacteroides cereus*.[138] Despite relatively well-conserved metal-binding sites, these enzymes share only marginal structural similarity and differ greatly in terms of substrate binding. The conversion of glyoxalase II into a β-lactamase was achieved through a series of extensive modifications involving insertion, deletion, and substitution of several active site loops and subsequent point mutations.[104] This redesign endeavor altered the metal binding geometry as well as the substrate-binding pocket, yet both glyoxalase II and metallo-β-lactamase enzymes contain binuclear metal ions essential to the hydrolysis reaction. Although a designed dinuclear zinc site is present in the de novo-designed due ferri (DF) family of proteins,[139] no activity has been reported for any dinuclear zinc site introduced into any de novo or preexisting metal scaffold that did not already contain a Zn_2 site.

Another approach to the design of zinc enzymes is to begin with a zinc protein that is not catalytically active at all, but in which the Zn(II) center serves solely a structural function, as it does for the ZF proteins.[105,106] Catalytic Zn(II) sites can be prepared by taking the existing structural site and removing a ligand to create an open coordination sphere for binding and

dx.doi.org/10.1021/bi4016617 | *Biochemistry* 2014, 53, 957−978

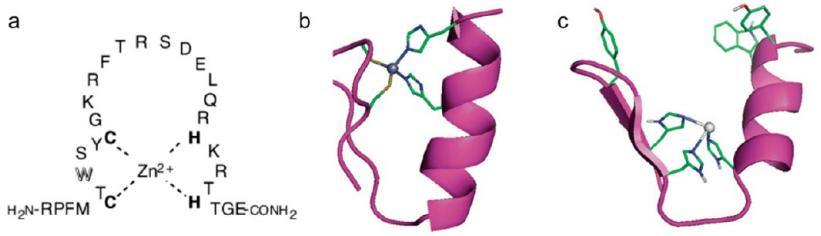

Figure 11. (a) Amino acid sequence of the zinc finger parent peptide. Panel a was reproduced from ref 105. Copyright 2004 American Chemical Society. (b) Natural zinc finger fold ($\alpha\beta\beta$ structure) and (c) zinc finger $\alpha\beta\beta$ fold modified as a metallohydrolase. Panels b and c were reproduced from ref 151. Copyright 2010 Elsevier.

Table 3. Active Site Properties of Carbonic Anhydrase II and Selected Mutants

	coordination site	K_d(Zn(II)) (pM)	pK_a of Zn-OH$_2$	CO$_2$ hydration k_{cat}/K_M (μM^{-1} s^{-1})	*p*NPA hydrolysis k_{cat}/K_M (M^{-1} s^{-1})
wild type	His$_3$(H$_2$O)	0.8 ± 0.1[a]	6.8 ± 0.1[b]	110 ± 10[c]	2600 ± 50[c]
			Primary Coordination-Sphere Mutants		
H94D[d,e]	His$_2$Asp	15000 ± 5000	≥9.6	0.11 ± 0.01	365 ± 70
H94A[e]	His$_2$	270000 ± 50000		0.012 ± 0.0002	18
H94C[e,f]	His$_2$Cys	33000 ± 7000	≥9.5	0.11 ± 0.01	117 ± 20
			Secondary Coordination-Sphere Mutants		
T199C[g,h]	His$_3$Cys	1.1 ± 0.2		0.11 ± 0.02	
T199D[i]	His$_3$Asp	4 ± 0.02		0.04 ± 0.005	
T199E[i]	His$_3$Glu	0.02 ± 0.01		0.04 ± 0.005	
T199H[i]	His$_3$(H$_2$O)	77 ± 13	≥9.0	0.024 ± 0.002	
T199A	His$_3$(H$_2$O)	60 ± 10[j]	8.3 ± 0.1[c]	1.1 ± 0.05[c]	44 ± 2[c] or 15[k]
E117Q[l]	His$_3$(H$_2$O)	4400 ± 400	≥9.0	0.002	3

[a]Taken from ref 120. Notably, recent ITC data revealed a K_d (0.5 nM) ~3 orders of magnitude weaker than prior values for CA.[119] However, for this discussion, we have chosen to use the stronger K_d value so that it can be uniformly compared to those of the mutants that have not been re-evaluated. [b]From ref 186. [c]From ref 169. [d]From ref 118. [e]From ref 117. [f]From ref 121. [g]From ref 123. [h]From ref 62. [i]From ref 124. [j]From ref 127. [k]From ref 125. [l]From ref 129.

activation of external ligands. This was first attempted by Merkle and co-workers, who reported a truncated ZF peptide, CP1-C4 (CP1, PYKCPECGKSFSQKSDLVKHQNTHTG) in which the last four residues (including a His) were removed, to create a peptide that binds Co(II) with a tetrahedral geometry.[140] Although evidence of an open coordination site was obtained by examining the spectra of Co(II)−peptide complexes with external ligands, neither Zn(II) or Co(II) complexes displayed any hydrolytic activity, a result proposed to be due to the high pK_a expected for a thiolate-rich site with no secondary interactions. Later, Nomura et al. reported the first successful attempt at redesigning the structural zinc center in a ZF [wild-type sequence of RPFMCTWSYCGKRFTRSD-ELQRHKRTHTGE, zf(CCHH)] into a hydrolytic Zn(II) site by preparing a series of ZF mutants in which one of the coordinating residues was substituted with a noncoordinating residue (Ala or Gly) (Figure 11a).[105,141,142] For those mutants retaining at least one Cys in the coordination sphere, Co(II) substitution indicated four- or five-coordinate geometries. The highest activity (*p*NPA hydrolysis) was observed for zf-(CCHA), which has a sequence similar to that of the truncated ZF CP1-C4 and four-coordinate geometry (with an open site) and a second-order rate constant of 0.568 ± 0.0228 M^{-1} s^{-1}. The zinc center is located in a more hydrophobic environment in zf(CCHA) than in CP1-C4[140] because of the presence of the C-terminal residues, which can affect both substrate binding and the acidity of the Zn(II)-bound water molecule.[143] All of the other mutants with at least one Cys in the coordination sphere were five-coordinate, including two vacant sites. Generally, ZFs of the CHH type displayed activities higher than those of the CCH type, probably because the Cys residue can decrease the Lewis acidity of the Zn(II) center via its electron donating ability and consequently reduce the activity (Table 3). To this end, the authors prepared several HHH-type ZFs, which should bind as neutral ligands (as in CA) and help maximize the Lewis acidity. As expected, increased activity was observed relative to those of the Cys-containing ZFs [up to 0.966 ± 0.0492 M^{-1} s^{-1} for zf(HHHH)]. While only rarely seen in nature (for example, a structural site in the HAP1 transcriptional factor[144]), a ZnHis$_4$ site has also been observed in a related redesigned ZF protein (although there are no structural data indicating whether additional solvent molecules are found in the coordination sphere)[145] and in the MBPC-2 system reported by Salgado et al.,[146] but no activity was reported for either. Co(II) substitution of all of these, however, indicated six-coordinate geometries with at least two vacant sites, but given the preference of Co(II) for octahedral geometries, lower coordination numbers for Zn(II) cannot be ruled out. The hydrolysis of *p*NPA as performed by these ZF mutant peptides is pH-dependent with pK_a values for Zn-OH$_2$ deprotonation ranging from 6.3 to 7.6 that increase according to the Lewis acidity of the Zn(II) center. The activity of the His$_4$ site falls within the range of activities reported for synthetic small molecule model complexes in mostly aqueous conditions[134−136,147,148] yet remains almost 3000-fold slower than CAII.[18,149] zf(HHHH) also displays nuclease activity toward substrates bis(*p*-nitrophenyl) phosphate and super-coiled plasmid DNA (pUC19GC).[150] Overall, this work further demonstrates the importance of having primarily neutral

dx.doi.org/10.1021/bi4016617 | *Biochemistry* 2014, 53, 957−978

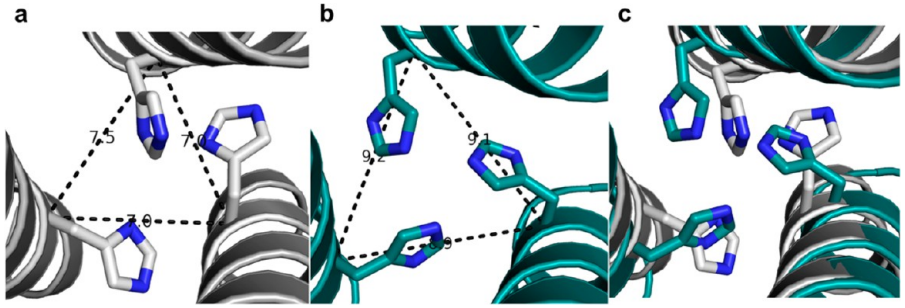

Figure 12. Comparison of the size of the active site cavities of (a) the modeled His_3 site using the structure of $[As(III)]_S(\mathbf{CS}L9C)_3$ (PDB entry 2JGO)[194] and (b) the actual structure containing the His_3 site, $[Hg(II)]_S[Zn(II)(H_2O/OH^-)]_N(\mathbf{CS}L9PenL23H)_3^{n+}$ (PDB entry 3PBJ).[152] (c) Overlay of the two sites with the model colored gray and the actual structure colored cyan. This figure was reproduced from ref 47. Copyright 2013 Elsevier.

ligands in the coordination spheres of Zn(II) centers in hydrolytic enzymes.

In another study, a ZF protein ($\alpha\beta\beta$ fold) was targeted for computational redesign as a hydrolase (Figure 11c).[151] In this design method, CYANA and then IDeAS were used to design a linker between D-amino acid-nucleated secondary structures (α-helix and two β-hairpins) and to optimize the sequence, respectively. The resulting small 21-mer sequence with $\alpha\beta\beta$ structure bound Zn(II) with a K_d of ~800 μM and a ΔG° of approximately −17.2 kJ mol^{-1}. Therefore, binding of Zn(II) to this His_3 site is weaker than for any of the other designs discussed above (Table 1). Hydrolysis of *p*NPA was observed with an initial rate of $(103.45 \pm 0.25) \times 10^{-9}$ M s^{-1}, a 45-fold enhancement over the background at pH 7.0 and 25 °C. However, enzymelike hydrolysis with substrate binding was not observed, possibly because the short sequence and small size of the fold do not provide sufficient protein structure to support substrate binding.

FROM ZINC-BINDING PROTEINS TO HYDROLYTIC METALLOENZYMES

Until recently, designed zinc metalloproteins have often shown very little, if any, catalytic activity relative to their natural counterparts and few have been structurally characterized. As discussed above, there are examples in which preexisting Zn(II) sites have been redesigned for different functions, such as converting glyoxalase II to a metallo-β-lactamase[104] and converting ZF peptides (closed coordination spheres) to catalytic sites by opening up the first coordination sphere,[140] but generating hydrolytic activity from a "new" zinc site in either a de novo or preexisting protein scaffold had not yet been achieved. In early 2012, we reported the first example of a hydrolytically active de novo-designed zinc site.[152] Soon after, Khare et al. reported the de novo computational redesign and subsequent directed evolution of a Zn(II)-containing mouse adenosine deaminase for efficiently catalyzing the hydrolysis of a model organophosphate substrate.[153] Not long after that, Der et al. reported the de novo design of a $ZnHis_3$ site at the computationally designed interface between two copies of the Rab4-binding domain of Rabenosyn, which effectively catalyzes the hydrolysis of both *p*NPA and *p*-nitrophenyl phosphate (*p*NPP).[95,96]

Here, we will emphasize our work on introducing a hydrolytic zinc site into a de novo-designed scaffold and provide detailed comparisons to these other hydrolytic zinc enzymes. Our original goal was to create a de novo-designed protein (a homomeric parallel 3SCC), which could bind two different metals in spatially separated sites, with different functions. The design of the parent coiled coil sequence [**TRI**, Ac-G(LKALEEK)$_n$G-NH_2][154,155] is based on the heptad repeat approach, consisting of seven amino acid repeats, labeled **a**−**g**. This sequence results in formation of amphipathic α-helices with all Leu residues in positions **a** and **d** to make up the hydrophobic face, Ala in position **c** as a helix inducer, and mostly Lys and Glu residues in the remaining hydrophilic positions. The resulting 3SCC structure (at pH >5.5, where stabilizing salt bridge interactions can be formed between the Lys and Glu residues) has Leu residues in positions **a** and **d** oriented toward the interior. Therefore, when residues such as His or Cys are substituted into these positions, metal-binding sites can be formed. The sequence chosen to achieve our original goal is **TRI**L9CL23H, where His at position 23 is intended for formation of a $ZnHis_3X$ site. In addition to the envisioned catalytic zinc site, we engineered a stabilizing structural site (HgS_3, where S represents a thiolate ligand) utilizing principles for heavy metal binding defined by earlier work in the group.[154,156−164] Having a structural site was initially desirable in part to support substitution of the bulky, potentially destabilizing, His residues into the interior of the coiled coil. X-ray crystallographic analysis does demonstrate some fraying of the coiled coil below the His site (Figure 12), and circular dichroism (CD) studies indicate somewhat lower α-helical content for His-containing peptides (~70−80%) than for those that contain single Cys substitutions (>90%). Hg(II) was specifically chosen for the structural site (Cys_3) for several reasons. Previous work had demonstrated that Hg(II) could be used to induce folding in an otherwise unfolded 3SCC.[156] Interestingly, although Hg(II) prefers to form a two-coordinate metal complex,[165,166] it not only induces folding in this system but also forms a stable three-coordinate Hg(II) site, only rarely observed.[154,155,167] Additionally, its high affinity for sulfur atoms ensures it will remain bound to the thiolate ligands, allowing Zn(II) to bind exclusively to the His_3 site. Finally, the spectroscopic properties of Hg(II) sites of varying coordination numbers have been well-characterized, allowing for a spectroscopic tag to assess trimer formation (this is especially important for our most recent work in which the position of His along the peptide sequence is varied[168]).

CD denaturation titrations quickly confirmed the function of the structurally stabilizing HgS_3 site [UV−vis spectroscopy also confirmed the trigonal binding nature of Hg(II) in the site].[152] The X-ray crystal structure of the Hg(II)- and Zn(II)-bound form of **CS**L9PenL23H (**CoilSer** or **CS**, sequence of Ac-E WEALEKK LAALESK LQALEKK LEALEHG-NH_2, is the

dx.doi.org/10.1021/bi4016617 | *Biochemistry* 2014, 53, 957−978

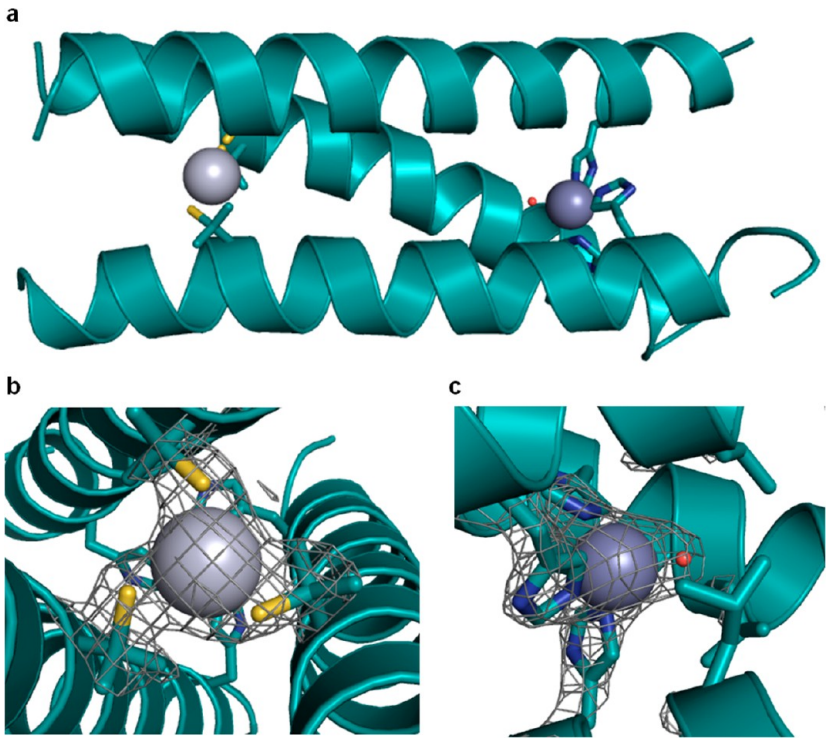

Figure 13. Ribbon diagrams of the $[Hg(II)]_S[Zn(II)(H_2O/OH^-)]_N(\mathbf{CS}L9PenL23H)_3^{n+}$ parallel 3SCC (one of two different three-helix bundles present in the asymmetric unit) at pH 8.5. Shown are the main chain atoms represented as helical ribbons (cyan) and the Pen and His side chains in stick form (yellow for sulfur, blue for nitrogen, and red for oxygen). (a) One of two trimers found in the asymmetric unit of the crystal structure. (b) Top-down view of the structural trigonal thiolate site, HgS_3, confirming the proposed structure of Hg(II) in Cys-containing **TRI** peptides.[154] This metal site should mimic well the structural site in the metalloregulatory protein MerR.[167] (c) Side view of the tetrahedral catalytic site, ZnN_3O, which closely mimics carbonic anhydrase and matrix metalloproteinase active sites.[195] All figures are shown with $2F_o - F_c$ electron density contoured at 1.5σ overlaid. This figure was reproduced from ref 152. Copyright 2012 Nature Publishing Group.

crystallographic analogue sequence of **TRI** and behaves similarly in solution) verified the geometry of the HgS_3 site and provided the first picture of the designed ZnN_3X site (where N represents a His ligand, Figure 13).[152] Although two individual trimers are present in the asymmetric unit of the structure, both have Zn(II) bound in a pseudotetrahedral geometry to three His residues and one chloride or water. The two sites overlay well with each other, and the ZnN_3O (where O represents water or hydroxide) site overlays extremely well with the active site of CAII (and with those of MMPs such as adamalysin II) (Figure 14). Despite the structural similarity, especially in the geometry of the first coordination sphere, there are several differences between this designed Zn(II) site within a coiled coil and CAII. The most noticeable distinction is that the secondary structure around the active sites is very different between the two: primarily β-sheets for CA and all α-helices for the design. Smaller differences exist in the relative orientation of the imidazole rings of the His residues, the identities of the coordinating nitrogens (ε vs δ), and, of course, the hydrogen bonding structure and water channels present in CA that have not been explicitly designed in the coiled coil (Figure 10). These differences can allow us to use this design to address one of the objectives of metalloprotein design, determining the minimal unit required to achieve the desired coordination environment and then, significant catalytic activity. Of course, the achievement of a Zn(II) site structurally similar to that in CA shows that this Zn(II) coordination environment can be achieved in diverse protein scaffolds, but a more challenging question is whether this minimal site is enough to confer significant enzymelike catalytic activity. Is it possible to remove an active site from a native metalloenzyme, put it into a wholly different (and smaller) protein structure, and preserve similar activity and properties? Can the minimal site be built up to match the native protein's catalytic power, by introducing increasing complexity along the way? Achievement of these goals will require a deep understanding of the structure–function relationships involved, gained through careful analyses of all designed systems.

To answer the first catalytic activity question, we chose to examine whether the designed metal–peptide complex could hydrolyze *p*NPA. Indeed, the minimal first coordination-sphere model $\{[Hg(II)]_S[Zn(II)(H_2O/OH^-)]_N(\mathbf{TRI}L9CL23H)_3^{n+}$, where the subscript S represents metal binding to the sulfur site, N is used for binding to the His site, and H_2O/OH^- refers to solvent coordinated to Zn(II) for which the protonation state varies depending on pH$\}$ exhibits saturation kinetics for *p*NPA hydrolysis in a pH-dependent manner with a measured k_{cat} of up to 0.04 s^{-1} at pH 9.5 and a k_{cat}/K_M of 23.3 M^{-1} s^{-1}.[152] Fitting the pH-dependent data (k_{cat}/K_M vs pH) yields a kinetic pK_a of 9.0 ± 0.1, presumably due to deprotonation of Zn(II)-bound water to hydroxide, and a maximal efficiency [assuming 100% active Zn(II)–hydroxide species] of 31 ± 4 M^{-1} s^{-1} (Table 4).[168] This is >500-fold higher than second-order rate constants for comparable small molecule model complexes[134−136] and within ~100-fold of the efficiency of CAII, the fastest of the α-CA isozymes.[18,149] As discussed above, many mutant CAs in which secondary interactions are removed suffer from reduced activity (such as T199A, in which the direct hydrogen bonding Thr199 residue is removed, resulting in an ~100-fold lower catalytic efficiency[125,169]). Therefore, although

dx.doi.org/10.1021/bi4016617 | *Biochemistry* 2014, 53, 957−978

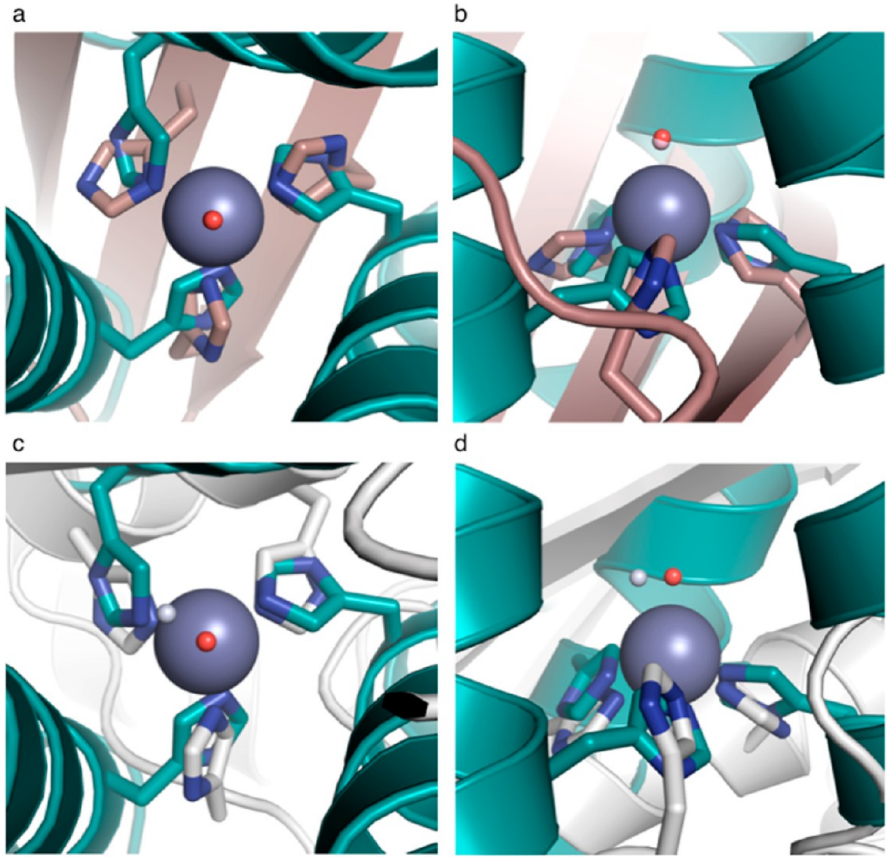

Figure 14. Overlay of the ZnN_3O site in $[Hg(II)]_S[Zn(II)(H_2O/OH^-)]_N(\mathbf{CS}L9PenL23H)_3^{n+}$ with the active site of human CAII and the matrix metalloproteinase (MMP) adamalysin II. $[Hg(II)]_S[Zn(II)(H_2O/OH^-)]_N(\mathbf{CS}L9PenL23H)_3^{n+}$ is colored cyan (PDB entry 3PBJ), CAII tan (PDB entry 2CBA), and adamalysin II gray (PDB entry 1IAG). (a) Top-down view of the overlay with CAII. The solvent molecule associated with $[Hg(II)]_S[Zn(II)(H_2O/OH^-)]_N(\mathbf{CS}L9PenL23H)_3^{n+}$ is colored red, and that associated with CAII lies underneath. (b) Side-on view of the overlay with CAII. The model displays an excellent structural overlay for the first coordination-sphere atoms with CAII; however, the orientation of the imidazoles differs between the two proteins. Another subtle difference is that the present structure has three ε-amino nitrogens bound to the Zn(II) ion whereas CAII has a mixed two-ε and one-δ coordination sphere. (c) Top-down view of the overlay with adamalysin II. The solvent molecule associated with adamalysin II is colored gray. (d) Side-on view of the overlay with adamalysin II. While the position of the His rings is close between the model and adamalysin II, the locations of the solvent molecules differ noticeably. Unlike for CAII, three ε-amino nitrogens bind to Zn(II) in adamalysin II.[193] The overlay was performed manually in PyMOL. This figure was adapted from ref 152.

Table 4. Properties of Zn(II)-His_3 Sites in TRI Peptides[a]

design complex	K_d(Zn(II)) (M) at pH 7.5[b]	K_d(Zn(II)) (M) at pH 9.0[c]	*p*NPA hydrolysis k_{cat}/K_M (M^{-1} s^{-1})[d]	K_M (mM)[e]	K_I (M)[f]
$[Zn(II)(H_2O/OH^-)]_N(\mathbf{TRI}L2WL23H)_3^{n+}$	0.6 ± 0.1	0.24 ± 0.02	25 ± 2	2.1 ± 0.2	0.34 ± 0.01
$[Hg(II)]_S[Zn(II)(H_2O/OH^-)]_N(\mathbf{TRI}L9CL23H)_3^{n+}$	0.8 ± 0.1	0.22 ± 0.06	31 ± 4	1.7 ± 0.5	0.32 ± 0.01
$[Zn(II)(H_2O/OH^-)]_N[Hg(II)]_S(\mathbf{TRI}L9HL23C)_3^{n+}$	~8	0.8 ± 0.3	24 ± 3	1.2 ± 0.2	0.20 ± 0.01
$[Hg(II)]_S[Zn(II)(H_2O/OH^-)]_N(\mathbf{TRI}L9CL19H)_3^{n+}$	3.7 ± 1.3	0.4 ± 0.2	27 ± 5	2.8 ± 0.4	0.36 ± 0.01

[a]From ref 168. [b]In 50 mM HEPES buffer and 0.1 M Na_2SO_4. [c]In 50 mM CHES buffer and 0.1 M Na_2SO_4. [d]Maximal k_{cat}/K_M assuming 100% Zn–hydroxide complex. [e]For *p*NPA hydrolysis at pH 9.5 in 50 mM CHES buffer and 0.1 M Na_2SO_4 at 25 °C. [f]Inhibition constant for *p*NPA hydrolysis by acetate at pH 8.5 in 50 mM CHES buffer and 0.1 M Na_2SO_4 at 25 °C.

this de novo-designed metalloenzyme is already within only ~100-fold of the fastest CA isozyme that has numerous conserved secondary interactions, removal of such interactions yields a mutant native protein with an efficiency that is approximately the same as that of a first-coordination-sphere-only model. Further, the kinetic parameters for the corresponding metal complex lacking the structural site, $[Zn(II)(H_2O/OH^-)]_N(\mathbf{TRI}L2WL23H)_3^{n+}$ (Figure 15), are similar (maximal k_{cat}/K_M = 25 ± 2 M^{-1} s^{-1}, and pK_a = 9.2 ± 0.1), confirming that the thermodynamic stability conferred by HgS_3 to the protein is not detrimental to the catalytic ZnN_3O site.[168] This is important for the design of multi-metal site proteins in which one may require different metals in different positions for different functions (e.g., one for catalysis and one for electron transfer). Additionally, the Zn(II) binding affinities for both complexes fall into the same range.[168] At pH 7.5, the K_d for binding of Zn(II) to $(\mathbf{TRI}L2WL23H)_3$ is 0.6 ± 0.1 μM and for $[Hg(II)]_S(\mathbf{TRI}L9CL23H)_3^{n-}$ is 0.8 ± 0.1 μM. The

dx.doi.org/10.1021/bi4016617 | *Biochemistry* 2014, 53, 957–978

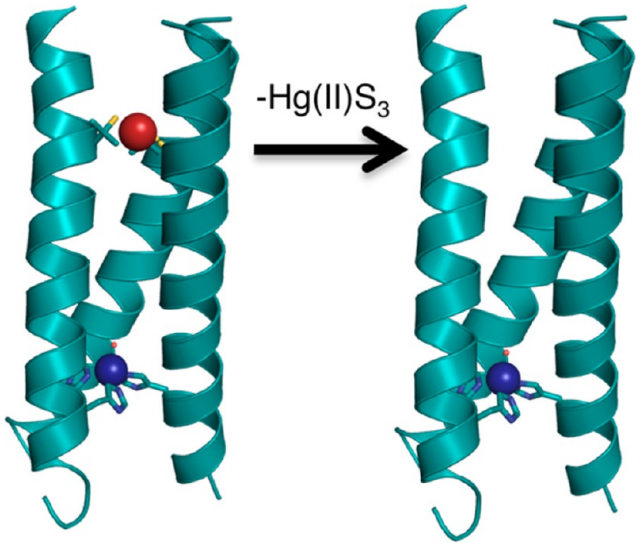

Figure 15. Comparison of the X-ray crystal structure of $[Hg(II)]_S[Zn(II)(H_2O/OH^-)]_N(\mathbf{CS}L9PenL23H)_3^{n+}$ (left, PDB entry 3PBJ)[152] with a PyMOL model of $[Zn(II)(H_2O/OH^-)]_N(\mathbf{TRI}L2WL23H)_3^{n+}$ lacking the HgS_3 structural site (right, based on PDB entry 3PBJ). This figure was reproduced from ref 168. Copyright 2013 American Chemical Society.

binding affinity increases at pH 9.0 to 0.24 ± 0.02 μM for the peptide lacking the structural site and to 0.22 ± 0.06 μM for $[Hg(II)]_S(\mathbf{TRI}L9CL23H)_3^{n-}$. These Zn(II) binding affinities fall into the range of those of designed Zn(II) proteins with metal sites made up of three protein ligands (Table 1).

We also chose to examine product inhibition of *p*NPA hydrolysis in our de novo-designed system. Acetate anion was used as the inhibitor because of its charge and relatively small size compared to those of the other *p*-nitrophenol/*p*-nitrophenolate (depending on pH) products. The competitive inhibition constants (K_I's) obtained at pH 8.5 for $[Hg(II)]_S[Zn(II)(H_2O/OH^-)]_N(\mathbf{TRI}L9CL23H)_3^{n+}$ and $[Zn(II)(H_2O/OH^-)]_N(\mathbf{TRI}L2WL23H)_3^{n+}$ are similar within error (0.32 ± 0.01 and 0.34 ± 0.01 M, respectively).[168] Notably, the concentration of acetate required to inhibit this reaction is quite high, demonstrating that product inhibition is not an issue for our model protein, despite its relatively small size compared to the sizes of native proteins, under the conditions of our experiments. This is contrary to synthetic small molecule model complexes, which often have issues with product inhibition. Further, it should be noted that the K_I for the designed system is also higher than that for CA (K_I = 0.085 M for noncompetitive acetate inhibition at pH 7.55).[170−172] Acknowledging the different inhibition mechanisms, we find this is likely due to the presence of a substrate-binding pocket in CA whereas the designed system does not have a discrete binding pocket and has tighter packing interactions around the Zn(II) center. In both systems, the inhibitory effect decreases with an increase in pH, presumably because of competition with hydroxide.

There are now several examples of designed hydrolytic enzymes. Although none are truly de novo with regard to the scaffold into which they were designed, there are two that may be considered de novo sites designed into preexisting native protein scaffolds (this excludes designs such as the redesigned ZF sites described earlier). The Baker group reported a computationally redesigned mouse adenosine deaminase with a $ZnHis_3Asp$ site (trigonal bipyramidal geometry with one open coordination site), which could catalyze hydrolysis of an organophosphate substrate, diethyl 7-hydroxycoumarinyl (DECP), with a catalytic efficiency of 9750 M^{-1} s^{-1} after directed evolution.[153] The wild-type enzyme showed no acceleration for DECP hydrolysis over buffer at <20 μM enzyme, suggesting a k_{cat}/K_M of ~10^{-3} M^{-1} s^{-1}. The template protein for this model, although also a hydrolytic Zn(II) enzyme, has distinct transition state geometry, leaving group character, and inherent reactivity at the substrate electrophilic center. Although the primary coordination environment around the metal has not been changed, this design demonstrates an effective approach to introducing new reactivity into an existing metalloenzyme without relying on preexisting activity and demonstrating the substantial effects that the surrounding protein structure can have on the activity of the "same" metal site. Despite the high hydrolytic activity, we cannot directly compare this system to ours given the different substrates and also the distinct coordination environments. However, the Kuhlman group later reported the design of a $ZnHis_3$ site at the interface between two copies of the Rab4-binding domain of Rabenosyn that can catalyze both *p*NPA and *p*NPP hydrolysis (Figure 16).[96] This work involved the use of computational

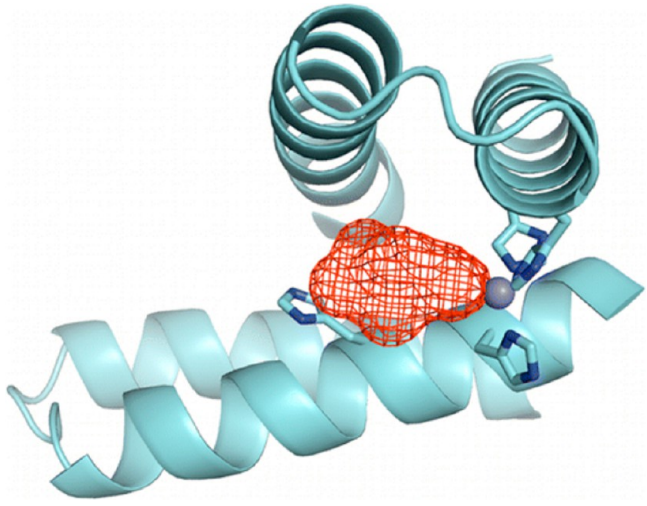

Figure 16. X-ray crystal structure of MID1-zinc, a designed protein with a metal-mediated protein interface. The red mesh represents the active site cleft above the open coordination site of the $ZnHis_3$ metal site. This figure was reproduced from ref 96. Copyright 2012 American Chemical Society.

methods to introduce a metal-binding site onto the surface of a monomeric protein to direct the formation of a dimer. Two His residues from one monomer and two from the other make up what was intended to be a $ZnHis_4$ site. The goal of the design was to use metal binding to improve the computational design of protein−protein interfaces, because metals can form stronger interactions with certain residues than simple protein−protein hydrogen bonds or van der Waals contacts.[95] The approach is similar to that taken by the Tezcan group, as discussed previously.[91,92,97] When the X-ray crystal structure unexpectedly revealed a $ZnHis_3$ site at the interface, with tartrate filling the open coordination site, the authors tested the system for hydrolytic activity. At pH 8.5, the designed Zn(II) homodimer catalyzes the hydrolysis of *p*NPA with a rate of 0.22 s^{-1} and a K_M of 0.47 mM. As for $[Hg(II)]_S[Zn(II)(H_2O/$

dx.doi.org/10.1021/bi4016617 | *Biochemistry* 2014, 53, 957−978

$OH^-)]_N(\mathbf{TRI}L9CL23H)_3^{n+}$, the rate of hydrolysis is pH-dependent, increasing with an increase in pH and MID1-Zn (metal interface design with zinc) has a kinetic pK_a of 8.2 ± 0.1 and a maximal efficiency of 630 ± 90 M^{-1} s^{-1}. The authors demonstrate that mutating some of the surrounding residues to Glu results in a closed coordination sphere and a corresponding loss of activity (supporting a Zn−OH^- mechanism). Product inhibition constants were not reported; however, given the relatively open metal site in this structure and the increased Lewis acidity of Zn(II), it is reasonable to expect this designed zinc site will be more strongly inhibited by acetate anion than $[Hg(II)]_S[Zn(II)(H_2O/OH^-)]_N(\mathbf{TRI}L9CL23H)_3^{n+}$. MID1-Zn can also effectively catalyze the hydrolysis of *p*NPP (14 M^{-1} s^{-1} at pH 8.5), although it is an intrinsically less reactive substrate. Notably, the K_M for this reaction is 40-fold lower (12 μM), probably because of electrostatic interactions between the positively charged active site and the negatively charged phosphate group. Product inhibition of this reaction would likely be even more potent than for *p*NPA because it is a dianionic phosphate product that could bind to Zn(II). The authors discuss the importance of an apolar substrate-binding cleft around the active Zn(II) center in achieving these efficiencies. The presence of tartrate in the crystal structure highlighted a binding pocket ∼6 Å wide and 4 Å deep around the open coordination site of the Zn(II) center. Many synthetic models are relatively ineffective given that they have no such binding cleft, although this can be improved somewhat in apolar solvents (and under micellar conditions), which can simulate the apolarity of an active site cleft.[173] The maximal efficiency of MID1-Zn is 20-fold higher than that of $[Hg(II)]_S[Zn(II)(H_2O/OH^-)]_N(\mathbf{TRI}L9CL23H)_3^{n+}$. One potential reason is the size of the active site; although there is room for substrate binding in $[Hg(II)]_S[Zn(II)(H_2O/OH^-)]_N(\mathbf{TRI}L9CL23H)_3^{n+}$, it is in a hydrophobic core and not open to solvent as is the interface site in MID1-Zn. Further, although we do not yet understand the source of the differences in the kinetic pK_a values, it has been suggested that the lower the pK_a, the more hydrolytically active the site will be [because Zn(II) will be a better Lewis acid].[143] Regardless, both designs display hydrolytic activity close to that of the fastest CA isozyme and competitive with both mutants of CAII and other CA isozymes with varying catalytic activities, making these the first examples of highly efficient designed metalloproteins with efficiencies that fall in the range expected for many native metalloenzymes. We have already discussed the possibilities of designing secondary hydrogen bonding interactions into $[Hg(II)]_S[Zn(II)(H_2O/OH^-)]_N(\mathbf{TRI}L9CL23H)_3^{n+}$, like Thr199 in CA, for matching the activity of the fastest isozyme; however, in the case of MID1-Zn, one may imagine that if the same increase in efficiency can be achieved by adding hydrogen bonding interactions, then in theory the design could surpass the activity of CAII.

Although examination of the hydrolysis of *p*NPA is informative, it is not equal to the native, evolved reaction of CA, CO_2 hydration. No other designed protein has yet reported CO_2 hydration, but we have shown that $[Hg(II)]_S[Zn(II)(H_2O/OH^-)]_N(\mathbf{TRI}L9CL23H)_3^{n+}$ can catalyze this reaction at pH 9.5 with an efficiency of ∼1.8 × 10^5 M^{-1} s^{-1} and a rate of ∼1800 s^{-1}.[152] These kinetic parameters represent a complex that is certainly faster than any previous structurally related small molecule model complex.[174−181] More significantly, this catalytic efficiency falls close (∼1.7-fold lower than that of CAIII and ∼60-fold lower than that of CAXIII) to the range of efficiencies achieved by nature with the different CA isozymes (k_{cat}/K_M ranging from 3.0 × 10^5 to 1.5 × 10^8 M^{-1} s^{-1}).[182] Further, the design remains only ∼500-fold less than CAII, which is the fastest of the CA isozymes, therefore representing the most rigorous criterion. These results make this the first hydrolytic metalloenzyme designed from scratch that is competitive with one of the most efficient known natural enzymes. This work clearly demonstrates that it is possible to remove the active site from a native enzyme, embed it into an entirely different and minimized fold while retaining a structured "proteinlike" environment, and still achieve significant catalytic activity similar to those of highly evolved native metalloenzymes.

Now that we have learned that a minimal model of the native enzyme's active site can achieve a significant amount of hydrolytic activity, we are interested in gaining the remaining few hundred-fold difference between our design and CAII. We have already discussed several design examples illustrating the importance of secondary interactions. Although we have successfully achieved a first-coordination-sphere model, we have yet to incorporate any of the many surrounding interactions that exist in CAII, mainly hydrogen bonding networks (Figure 10). When we compare our model with mutant CAs, such as the T199A mutant [where the hydrogen bond to the Zn(II)-coordinating solvent molecule has been removed], little to no difference in efficiency is observed. Approximately 100-fold is lost for the CAII T199A mutant for both *p*NPA hydrolysis and CO_2 hydration, although the importance of the full hydrogen bond network including Thr199 and also Glu106, as described earlier, should be recognized because it is likely that more than a single hydrogen bond will be needed.[125,169] Further, the pK_a for these mutants can increase by 1.5−2 pH units, reaching that of the model. Therefore, it will be necessary to incorporate secondary interactions into this designed system. However, the attainment of hydrogen bonding channels such as those that would be required may be dependent on the location of the metal site in the 3SCC and other considerations, such as solvent and substrate access and metal binding affinities. To this end, we chose to first examine how the location of our minimal active site model may affect the catalytic efficiency for *p*NPA hydrolysis, kinetic pK_a, solvent and substrate access, rate, and Zn(II) binding affinities.[168] Few studies have taken a similar approach in which the location of a single metal-binding site is varied throughout a designed structure.[84,85,183] One example of a de novo protein in which this was done resulted in only one well-folded scaffold that demonstrated a 1:1 binding stoichiometry for Zn(II) to the protein (DS119 with $\beta\alpha\beta$ structure, as described earlier in this Current Topic).[85] The redesign of Trx to incorporate a $ZnHis_2Cys_2$ site discussed earlier is an example in which the location of the site was varied and used to compare the effects on metal binding affinity and structural stability.[84] Another example in which the effects of site location on catalysis were examined also involved the redesign of Trx, this time for the incorporation of a mononuclear non-heme iron site for superoxide dismutase function.[183] In both cases, the location of the site was observed to have significant effects on metal binding [for Zn(II)] and function (for the iron site).

We chose to perform complete kinetic analyses on two other sequences. The first was **TRI**L9HL23C, in which the catalytic site has been moved from the C-terminus to the N-terminus (Figure 17b).[168] The anticipated difference in this design is the

dx.doi.org/10.1021/bi4016617 | *Biochemistry* 2014, 53, 957−978

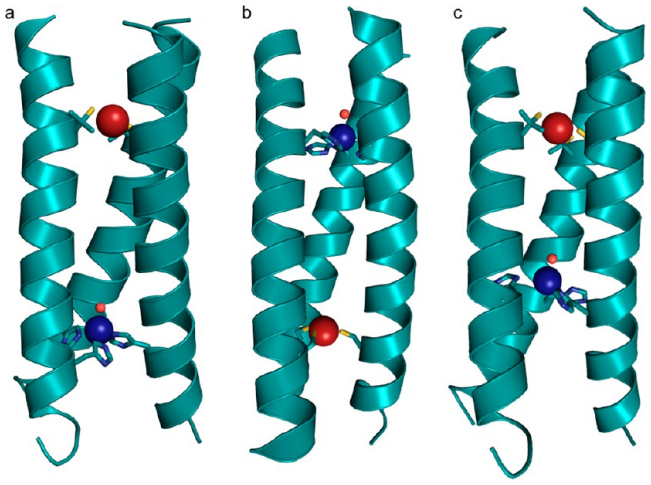

Figure 17. Comparison of the X-ray crystal structure of (a) $[Hg(II)]_S[Zn(II)(H_2O/OH^-)]_N(\mathbf{CS}L9PenL23H)_3^{n+}$ (PDB entry 3PBJ)[152] with PyMOL models of (b) $[Zn(II)(H_2O/OH^-)]_N[Hg(II)]_S(\mathbf{TRI}L9HL23C)_3^{n+}$ based on the coordinates of PDB entry 2JGO[194] and (c) $[Hg(II)]_S[Zn(II)(H_2O/OH^-)]_N(\mathbf{TRI}L9CL19H)_3^{n+}$ based on the coordinates of PDB entry 3PBJ. Models were prepared in PyMOL using the mutagenesis option and PyMOL's rotamer library.[196] This figure was adapted from ref 168.

relative exposure of the open coordination site on Zn(II) to the solvent. According to the crystal structure of $[Hg(II)]_S[Zn(II)(H_2O/OH^-)]_N(\mathbf{CS}L9PenL23H)_3^{n+}$, the coordinated solvent molecule in the Zn(II) active site is oriented toward the N-terminus, or into the hydrophobic interior of the 3SCC. Assuming the orientation of the site remains constant when moved from position 23 to position 9, we may expect the coordinated solvent molecule to continue pointing toward the N-terminus, but given its shorter distance from position 9, it may be more exposed to the solvent. Indeed, kinetic analysis of *p*NPA hydrolysis by this complex yields a reduced K_M (from ∼2 to ∼1 mM for the L23H sites), representative of increased substrate access (Table 4). The kinetic pK_a has not changed (9.2 ± 0.1), suggesting that the Lewis acidity has not been altered relative to that of the L23H site, and the maximal catalytic efficiency is approximately the same (24 ± 3 M^{-1} s^{-1}); however, the rate has also decreased ∼50% (to 0.020 ± 0.002 s^{-1}) relative to that of $[Hg(II)]_S[Zn(II)(H_2O/OH^-)]_N(\mathbf{TRI}L9CL23H)_3^{n+}$ at pH 9.5 (0.04 ± 0.01 s^{-1}). The Zn(II) binding affinity for this "upside-down" peptide is also decreased, ∼10-fold relative to that of $[Hg(II)]_S[Zn(II)(H_2O/OH^-)]_N(\mathbf{TRI}L9CL23H)_3^{n+}$ at pH 7.5 (K_d ∼ 8 μM) and by ∼4-fold at pH 9.0 (K_d = 0.8 ± 0.3 μM). While the K_M suggests our hypothesis of increasing substrate access by moving the site to position 9 is correct, another method was needed for validation. To this end, we studied the product inhibition for *p*NPA hydrolysis using the acetate anion at pH 8.5, as described above for $[Hg(II)]_S[Zn(II)(H_2O/OH^-)]_N(\mathbf{TRI}L9CL23H)_3^{n+}$ (K_I = 0.32 ± 0.01 M) and $[Zn(II)(H_2O/OH^-)]_N(\mathbf{TRI}L2WL23H)_3^{n+}$ (K_I = 0.34 ± 0.01 M). While these are equivalent within the error, that obtained for $[Zn(II)(H_2O/OH^-)]_N[Hg(II)]_S(\mathbf{TRI}L9HL23C)_3^{n+}$ decreases to 0.20 ± 0.01 M, providing stronger evidence for increased levels of solvent, substrate, and now inhibitor access to the Zn(II) site at position 9. Despite this increased level of access to the active Zn(II) site, the kinetic pK_a suggests the Lewis acidity has not changed relative to that of the L23H sites, implying that site access may not play a large role in tuning pK_a values in this system.

The next sequence we designed to study the effects of position on the active site is **TRI**L9CL19H.[168] In this sequence, the active site is also moved closer to the N-terminus, but only by a few residues, from an **a** position to a **d** position in the heptad repeat and also further into the interior of the 3SCC (Figure 17c). Because various thiolate conformations of Cys residues (in **a** vs **d** sites) in the **TRI** peptides have strongly affected the pK_a's for Cd(II), Hg(II), and Pb(II) binding,[158,184,185] we hypothesized that similar behavior could occur with His residue substitutions and Zn(II) binding. Also, moving the site further into the interior could affect the hydrophobicity surrounding the site, the substrate access, and the folding of the entire complex. CD studies confirmed that **TRI**L9CL19H remained well-folded despite moving the large His residues closer to the center of the assembly. The binding affinity of Zn(II) for $[Hg(II)]_S(\mathbf{TRI}L9CL19H)_3^{n-}$ falls between those for the L23H sites and the L9H site and follows the same trend with pH (K_d of 3.7 ± 1.3 μM at pH 7.5 and 0.4 ± 0.2 μM at pH 9.0). The maximal catalytic efficiency for *p*NPA hydrolysis is approximately the same as the others, 27 ± 5 M^{-1} s^{-1}, but the pK_a has increased to 9.6 ± 0.1 (Table 4). This increase may be due to altering the conformation of the His residues or because the metal site has been moved farther into the interior of the 3SCC. The K_M has slightly increased to ∼2.5 mM, and the maximal k_{cat} is now estimated to be ∼0.076 s^{-1} (relative to an average of ∼0.054 s^{-1} for the L23H sites and only ∼0.030 s^{-1} for L9H). The acetate inhibition constant is approximately the same as for the L23H sites, 0.36 ± 0.01 M.

Overall, the position of the Zn(II) active site along the 3SCC affects the binding affinities; rates; substrate, solvent, and inhibitor access; and kinetic pK_a values but does not collectively change the overall catalytic efficiency significantly. A relatively small ∼10-fold variation is observed in the binding affinities between each of the sites, consistent with other designed proteins, supporting a potential limit to the affinity that can be achieved with three protein ligands and no further stabilizing interactions. The kinetic pK_a is highest for the site most central to the 3SCC, although all of the pK_a values remain at least 2 units higher than that for CAII (6.8).[186] The catalytic rates follow a trend, where the lowest maximal k_{cat} is observed for the most solvent-accessible site in **TRI**L9HL23C and the highest for the probably least solvent-accessible site in **TRI**L9CL19H. It is an important finding for protein design that simply moving the active site along the sequence of a helical structure can control solvent and substrate accessibility while not diminishing the maximal catalytic efficiency. These modifications can potentially be used to control substrate selectivity, a desirable feature of native enzymes. Regardless of these differences, the overall catalytic efficiency for the metal complex of each sequence is retained, suggesting that this minimal first-coordination-sphere Zn(II) site in a helical structure is all that is required to attain significant hydrolytic activity. This is especially important for the next steps of this design series involving the incorporation of hydrogen bonding channels and stabilizing secondary interactions because one can alter the position of the active site to maximize the potential for such interactions.

■ CONCLUSIONS

The methodology for attaining a stable mononuclear Zn(II) site with the desired coordination geometry is now well-

dx.doi.org/10.1021/bi4016617 | *Biochemistry* 2014, 53, 957−978

established, although there is minimal success at incorporating second-sphere interactions.[116,187] Recent work has provided several examples of designed hydrolytic zinc enzymes, prepared through a variety of routes and leading to a deeper understanding of the structure−function relationship in zinc metalloproteins. On the basis of our de novo-designed system, it seems that a significant amount of hydrolytic activity can be achieved by simply harnessing the inherent catalytic power of Zn(II) within a well-defined protein structure (coiled coils). A first-coordination-sphere match, in which the binding ligands are three neutral His residues, is enough to achieve a modest binding affinity (K_d on the order of $\sim 10^{-6}$ M) and substantial catalytic activity, and only small variations are observed depending on the surrounding structure. The current challenge is to fine-tune such sites so as to match the properties of native zinc enzymes fully with higher binding affinities, kinetic pK_a values in a physiological pH range, and higher catalytic activities. Mutagenesis studies of native enzymes have clearly indicated the importance of surrounding hydrogen bonding networks to all active site properties, and CA, in particular, has proven to be a powerful model enzyme for understanding the effects of many of these interactions. However, similar first coordination spheres are found in a variety of different proteins with various functions, and native enzymes can often accommodate a mutation by replacing the lost residue with a similar interaction, indicating that the bulk of the protein matrix in native proteins can hide potentially important structural features and patterns. Now that primary Zn(II) sites can be modeled in small, stable designed protein scaffolds with efficient enzymelike hydrolytic activities, the feat of truly building a mononuclear zinc enzyme from the bottom up, uncovering these hidden structural features, and including specific hydrogen bonding networks and substrate selectivity, may be addressed.

Here we have highlighted the presence of similar binding sites in proteins across a range of zinc enzymes (with an emphasis on the $ZnHis_3$ site), but it should be recognized that these $MHis_3$ sites are also present in other metalloproteins, including those with redox activity. Specifically, $CuHis_3$ sites are found in enzymes such as peptidylglycine α-hydroxylating monooxygenase (for electron transfer),[188] Cu nitrite reductase (CuNiR, for redox catalysis),[189] and amine oxidase[190] and quercetin 2,3-dioxygenase[191] (for O_2 activation). It is intriguing that a metal site with the same primary structure in three different enzymes can be tuned for this variety of functions. Unlike hydrolytic sites, redox sites are more challenging to design as one must account for the structural changes associated with changing metal oxidation states. We have reported the design and characterization of a $CuHis_3$ site in the same scaffold as described earlier for Zn(II) binding in the absence of a structural site (**TRI**L2WL23H).[192] While both Cu(I) and Cu(II) complexes are formed and have been well-characterized, these do not appear to model the coordination geometries of native copper enzymes like CuNiR as faithfully as the corresponding designed $ZnHis_3$ site does for CA. Further, while catalytic activity relevant to the CuNiR system can be achieved, it is $\sim 10^7$-fold lower than that of native CuNiR, whereas the designed Zn(II) system is only $\sim 10^2$-fold less efficient than native CA. This illustrates two important points. Hydrolytic Zn(II) sites will, in general, be more amenable to design strategies as only one oxidation level needs to be accurately reproduced, and simply placing the three minimal His residues into a protein environment does not ensure that high activity will be achieved in every case, with every metal. From this perspective, the development of a deep understanding of and attention to the secondary coordination environment is likely critical for the most successful metalloprotein design.

AUTHOR INFORMATION

Corresponding Author

*E-mail: vlpec@umich.edu. Telephone: (734) 763-1519.

Present Address

[†]M.L.Z.: Department of Chemistry, Massachusetts Institute of Technology, Cambridge, MA 02139.

Funding

V.L.P. thanks the National Institutes of Health for support of this research (ES012236). M.L.Z. thanks the National Institutes of Health Chemistry-Biology Interface Training Program and the University of Michigan Rackham Graduate School for support of this research.

Notes

The authors declare no competing financial interest.

ABBREVIATIONS

CA, carbonic anhydrase; PDB, Protein Data Bank; *p*NPA, *p*-nitrophenyl acetate; MMP, matrix metalloproteinase; ITC, isothermal titration calorimetry; ZF, zinc finger; Bpy-Ala, (2,2′-bipyridin-5-yl)alanine; 3SCC, three-stranded coiled coil; Trx, thioredoxin; MBPC, metal binding protein complex; Phen, 1,10′-phenanthroline; DF, due ferri; *p*NPP, *p*-nitrophenyl phosphate; CD, circular dichroism; CS, CoilSer; DECP, diethyl 7-hydroxycoumarinyl; MID1-Zn, metal interface design with zinc; CuNiR, copper nitrite reductase.

REFERENCES

(1) Andreini, C., Banci, L., Bertini, I., and Rosato, A. (2006) Counting the Zinc-Proteins Encoded in the Human Genome. *J. Proteome Res. 5*, 196−201.

(2) Sousa, S. F., Lopes, A. B., Fernandes, P. A., and Ramos, M. J. (2009) The Zinc Proteome: A Tale of Stability and Functionality. *Dalton Trans.*, 7946−7956.

(3) Keilin, D., and Mann, T. (1939) Carbonic Anhydrase. *Nature 144*, 442−443.

(4) Vallee, B. L., and Neurath, H. (1954) Carboxypeptidase, a Zinc Metalloprotein. *J. Am. Chem. Soc. 76*, 5006−5007.

(5) Vallee, B. L. (1959) Biochemistry, Physiology and Pathology of Zinc. *Physiol. Rev. 39*, 443−490.

(6) Vallee, B. L., and Auld, D. S. (1990) Zinc Coordination, Function, and Structure of Zinc Enzymes and Other Proteins. *Biochemistry 29*, 5647−5659.

(7) Auld, D. S. (2001) Zinc Coordination Sphere in Biochemical Zinc Sites. *BioMetals 14*, 271−313.

(8) Gomis-Rüth, F. X., Stöcker, W., Huber, R., Zwilling, R., and Bode, W. (1993) Refined 1.8 Å X-ray Crystal Structure of Astacin, a Zinc-Endopeptidase from the Crayfish *Astacus astacus* L. Structure Determination, Refinement, Molecular Structure and Comparison with Thermolysin. *J. Mol. Biol. 229*, 945−968.

(9) Sträter, N., Klabunde, T., Tucker, P., Witzel, H., and Krebs, B. (1995) Crystal Structure of a Purple Acid Phosphatase Containing a Dinuclear Fe(III)-Zn(II) Active Site. *Science 268*, 1489−1492.

(10) Lesburg, C. A., Huang, C., Christianson, D. W., and Fierke, C. A. (1997) Histidine → Carboxamide Ligand Substitutions in the Zinc Binding Site of Carbonic Anhydrase II Alter Metal Coordination Geometry but Retain Catalytic Activity. *Biochemistry 36*, 15780−15791.

(11) McCall, K. A., Huang, C., and Fierke, C. A. (2000) Function and Mechanism of Zinc Metalloenzymes. *J. Nutr. 130*, 1437S−1446S.

(12) Emsley, J. (2001) Zinc. In *Nature's Building Blocks: An A-Z Guide to the Elements*, pp 499−505, Oxford University Press, Oxford, England.
(13) Andreini, C., Bertini, I., and Cavallaro, G. (2011) Minimal Functional Sites Allow a Classification of Zinc Sites in Proteins. *PLoS One 6*, e26325.
(14) Sigel, H., and Martin, R. B. (1994) The Colourless "Chameleon" or the Peculiar Properties of Zn^{2+} in Complexes in Solution. Quantification of Equilibria Involving a Change of the Coordination Number of the Metal Ion. *Chem. Soc. Rev. 23*, 83−91.
(15) Vallee, B. L., and Auld, D. S. (1993) New Perspective on Zinc Biochemistry: Cocatalytic Sites in Multi-Zinc Enzymes. *Biochemistry 32*, 6493−6500.
(16) Maret, W., and Li, Y. (2009) Coordination Dynamics of Zinc in Proteins. *Chem. Rev. 109*, 4682−4707.
(17) Maret, W. (2012) New Perspectives of Zinc Coordination Environments in Proteins. *J. Inorg. Biochem. 111*, 110−116.
(18) Verpoorte, J. A., Mehta, S., and Edsall, J. T. (1967) Esterase Activities of Human Carbonic Anhydrases B and C. *J. Biol. Chem. 242*, 4221−4229.
(19) Gould, S. M., and Tawfik, D. S. (2005) Directed Evolution of the Promiscuous Esterase Activity of Carbonic Anhydrase II. *Biochemistry 44*, 5444−5452.
(20) Wouters, M. A., and Husain, A. (2001) Changes in Zinc Ligation Promote Remodeling of the Active Site in the Zinc Hydrolase Superfamily. *J. Mol. Biol. 314*, 1191−1207.
(21) Auld, D. S. (2001) Zinc Sites in Metalloenzymes and Related Proteins. In *Handbook on Metalloproteins* (Bertini, I., Sigel, A., and Sigel, H., Eds.) pp 881−959, Marcel Dekker, New York.
(22) Matthews, B. W. (1988) Structural Basis of the Action of Thermolysin and Related Zinc Peptidases. *Acc. Chem. Res. 21*, 333−340.
(23) Rees, D. C., Lewis, M., and Lipscomb, W. N. (1983) Refined Crystal Structure of Carboxypeptidase A at 1.54 Å Resolution. *J. Mol. Biol. 168*, 367−387.
(24) Christianson, D. W., and Fierke, C. A. (1996) Carbonic Anhydrase: Evolution of the Zinc Binding Site by Nature and by Design. *Acc. Chem. Res. 29*, 331−339.
(25) Cheng, X., Zhang, X., Pflugrath, J. W., and Studier, F. W. (1994) The Structure of Bacteriophage T7 Lysozyme, a Zinc Amidase and an Inhibitor of T7 RNA Polymerase. *Proc. Natl. Acad. Sci. U.S.A. 91*, 4034−4038.
(26) Eklund, H., Nordström, B., Zeppezauer, E., Söderlund, G., Ohlsson, I., Boiwe, T., Söderberg, B. O., Tapia, O., Brändén, C. I., and Akeson, A. (1976) Three-Dimensional Structure of Horse Liver Alcohol Dehydrogenase at 2.4 Å Resolution. *J. Mol. Biol. 102*, 27−59.
(27) Erskine, P. T., Senior, N., Awan, S., Lambert, R., Lewis, G., Tickle, I. J., Sarwar, M., Spencer, P., Thomas, P., Warren, M. J., et al. (1997) X-Ray Structure of 5-Aminolaevulinate Dehydratase, a Hybrid Aldolase. *Nat. Struct. Biol. 4*, 1025−1031.
(28) Erskine, P. T., Norton, E., Cooper, J. B., Lambert, R., Coker, A., Lewis, G., Spencer, P., Sarwar, M., Wood, S. P., Warren, M. J., et al. (1999) X-Ray Structure of 5-Aminolevulinic Acid Dehydratase from *Escherichia coli* Complexed with the Inhibitor Levulinic Acid at 2.0 Å Resolution. *Biochemistry 38*, 4266−4276.
(29) Supuran, C. T. (2008) Carbonic Anhydrases: Novel Therapeutic Applications for Inhibitors and Activators. *Nat. Rev. Drug Discovery 7*, 168−181.
(30) Supuran, C. T., Di Fiore, A., Alterio, V., Monti, S. M., and De Simone, G. (2010) Recent Advances in Structural Studies of the Carbonic Anhydrase Family: The Crystal Structure of Human CA IX and CA XIII. *Curr. Pharm. Des. 16*, 3246−3254.
(31) Imtaiyaz Hassan, M., Shajee, B., Waheed, A., Ahmad, F., and Sly, W. S. (2013) Structure, Function and Applications of Carbonic Anhydrase Isozymes. *Bioorg. Med. Chem. 21*, 1570−1582.
(32) Namuswe, F., and Berg, J. M. (2012) Secondary Interactions Involving Zinc-Bound Ligands: Roles in Structural Stabilization and Macromolecular Interactions. *J. Inorg. Biochem. 111*, 146−149.
(33) Håkansson, K., Carlsson, M., Svensson, L. A., and Liljas, A. (1992) Structure of Native and Apo Carbonic Anhydrase II and Structure of Some of Its Anion-Ligand Complexes. *J. Mol. Biol. 227*, 1192−1204.
(34) Chang, X., Jorgensen, A. M., Bardrum, P., and Led, J. J. (1997) Solution Structures of the R6 Human Insulin Hexamer. *Biochemistry 36*, 9409−9422.
(35) Fujinaga, M., and James, M. N. (1987) Rat Submaxillary Gland Serine Protease, Tonin. Structure Solution and Refinement at 1.8 Å Resolution. *J. Mol. Biol. 195*, 373−396.
(36) Banerjee, S., Wei, B., Bhattacharyya-Pakrasi, M., Pakrasi, H. B., and Smith, T. J. (2003) Structural Determinants of Metal Specificity in the Zinc Transport Protein ZnuA from *Synechocystis* 6803. *J. Mol. Biol. 333*, 1061−1069.
(37) Parkin, G. (2004) Synthetic Analogues Relevant to the Structure and Function of Zinc Enzymes. *Chem. Rev. 104*, 699−767.
(38) DeGrado, W. F., Summa, C. M., Pavone, V., Nastri, F., and Lombardi, A. (1999) De Novo Design and Structural Characterization of Proteins and Metalloproteins. *Annu. Rev. Biochem. 68*, 779−819.
(39) Lu, Y., Berry, S. M., and Pfister, T. D. (2001) Engineering Novel Metalloproteins: Design of Metal-Binding Sites into Native Protein Scaffolds. *Chem. Rev. 101*, 3047−3080.
(40) Barker, P. D. (2003) Designing Redox Metalloproteins from Bottom-up and Top-down Perspectives. *Curr. Opin. Struct. Biol. 13*, 490−499.
(41) Kaplan, J., and DeGrado, W. F. (2004) De Novo Design of Catalytic Proteins. *Proc. Natl. Acad. Sci. U.S.A. 101*, 11566−11570.
(42) Lu, Y. (2006) Metalloprotein and Metallo-DNA/RNAzyme Design: Current Approaches, Success Measures, and Future Challenges. *Inorg. Chem. 45*, 9930−9940.
(43) Harris, K. L., Lim, S., and Franklin, S. J. (2006) Of Folding and Function: Understanding Active-Site Context through Metalloenzyme Design. *Inorg. Chem. 45*, 10002−10012.
(44) Koder, R. L., and Dutton, P. L. (2006) Intelligent Design: The de Novo Engineering of Proteins with Specified Functions. *Dalton Trans.*, 3045−3051.
(45) Lu, Y., Yeung, N., Sieracki, N., and Marshall, N. M. (2009) Design of Functional Metalloproteins. *Nature 460*, 855−862.
(46) Nanda, V., and Koder, R. L. (2010) Designing Artificial Enzymes by Intuition and Computation. *Nat. Chem. 2*, 15−24.
(47) Zastrow, M. L., and Pecoraro, V. L. (2013) Designing Functional Metalloproteins: From Structural to Catalytic Metal Sites. *Coord. Chem. Rev. 257*, 2565−2588.
(48) Yu, F., Cangelosi, V. M., Zastrow, M. L., Tegoni, M. M., Plegaria, J. S., Tebo, A. G., Mocny, C. S., Ruckthong, L., Qayuum, H., and Pecoraro, V. L. (2014) Protein Design: Towards Functional Metalloenzymes. *Chem. Rev.*, accepted for publication.
(49) Schurer, G., and Clark, T. (2009) The Reaction Mechanisms of Zinc Enzymes. *Patai's Chemistry of Functional Groups*, pp 1−29, Wiley, New York.
(50) Galdes, A. (1981) Zinc Metalloenzymes. In *Inorganic Biochemistry* (Hill, H. A. O., Ed.) pp 216−248, The Royal Society of Chemistry, London.
(51) Liang, J. Y., and Lipscomb, W. N. (1988) Hydration of Carbon Dioxide by Carbonic Anhydrase: Intramolecular Proton Transfer Between Zinc-Bound Water and Histidine 64 in Human Carbonic Anhydrase II. *Biochemistry 27*, 8676−8682.
(52) Lu, D., and Voth, G. A. (1998) Proton Transfer in the Enzyme Carbonic Anhydrase: An Ab Initio Study. *J. Am. Chem. Soc. 120*, 4006−4014.
(53) Christianson, D. W., Lipscomb, W. N., and Carboxypeptidase, A. (1989) *Acc. Chem. Res. 22*, 62−69.
(54) Jaffe, E. K. (2004) The Porphobilinogen Synthase Catalyzed Reaction Mechanism. *Bioorg. Chem. 32*, 316−325.
(55) Ryde, U. (1994) The Coordination Chemistry of the Catalytic Zinc Ion in Alcohol Dehydrogenase Studied by Ab Initio Quantum Chemical Calculations. *Int. J. Quantum Chem. 52*, 1229−1243.

(56) Myers, L. C., Terranova, M. P., Ferentz, A. E., Wagner, G., and Verdine, G. L. (1993) Repair of DNA Methylphosphotriesters through a Metalloactivated Cysteine Nucleophile. *Science 261*, 1164−1167.
(57) Penner-Hahn, J. (2007) Zinc-Promoted Alkyl Transfer: A New Role for Zinc. *Curr. Opin. Chem. Biol. 11*, 166−171.
(58) Handel, T., and DeGrado, W. F. (1990) De Novo Design of a Zn^{2+}-Binding Protein. *J. Am. Chem. Soc. 112*, 6710−6711.
(59) Pessi, A., Bianchi, E., Crameri, A., Venturini, S., Tramontano, A., and Sollazzo, M. (1993) A Designed Metal-Binding Protein with a Novel Fold. *Nature 362*, 367−369.
(60) Handel, T. T., Williams, S. A., and DeGrado, W. F. (1993) Metal Ion-Dependent Modulation of the Dynamics of a Designed Protein. *Science 261*, 879−885.
(61) Hitomi, Y., Outten, C. E., and O'Halloran, T. V. (2001) Extreme Zinc-Binding Thermodynamics of the Metal Sensor/Regulator Protein, ZntR. *J. Am. Chem. Soc. 123*, 8614−8615.
(62) Kiefer, L. L., Krebs, J. F., Paterno, S. A., and Fierke, C. A. (1993) Engineering a Cysteine Ligand into the Zinc Binding Site of Human Carbonic Anhydrase II. *Biochemistry 32*, 9896−9900.
(63) McCall, K. A., and Fierke, C. A. (2004) Probing Determinants of the Metal Ion Selectivity in Carbonic Anhydrase Using Mutagenesis. *Biochemistry 43*, 3979−3986.
(64) Maret, W. (2003) Cellular Zinc and Redox States Converge in the Metallothionein/Thionein Pair. *J. Nutr. 133*, 1460s−1462s.
(65) Müller, H. N., and Skerra, A. (1994) Grafting of a High-Affinity Zn(II)-Binding Site on the β-Barrel of Retinol-Binding Protein Results in Enhanced Folding Stability and Enables Simplified Purification. *Biochemistry 33*, 14126−14135.
(66) Schmidt, A. M., Müller, H. N., and Skerra, A. (1996) A Zn(II)-Binding Site Engineered into Retinol-Binding Protein Exhibits Metal-Ion Specificity and Allows Highly Efficient Affinity Purification with a Newly Designed Metal Ligand. *Chem. Biol. 3*, 645−653.
(67) Vita, C., Roumestand, C., Toma, F., and Ménez, A. (1995) Scorpion Toxins as Natural Scaffolds for Protein Engineering. *Proc. Natl. Acad. Sci. U.S.A. 92*, 6404−6408.
(68) Lindskog, S., and Nyman, P. O. (1964) Metal-Binding Properties of Human Erythrocyte Carbonic Anhydrases. *Biochim. Biophys. Acta 85*, 462−474.
(69) Regan, L., and Clarke, N. D. (1990) A Tetrahedral Zinc(II)-Binding Site Introduced into a Designed Protein. *Biochemistry 29*, 10878−10883.
(70) Klemba, M., and Regan, L. (1995) Characterization of Metal Binding by a Designed Protein: Single Ligand Substitutions at a Tetrahedral Cys_2His_2 Site. *Biochemistry 34*, 10094−10100.
(71) Bennett, B. (2010) EPR of Cobalt-Substituted Zinc Enzymes. In *Metals in Biology* (Hanson, G., and Berliner, L., Eds.) Vol. *29*, pp 345−370, Springer, New York.
(72) Gockel, P., Vahrenkamp, H., and Zuberbuhler, A. D. (1993) Zine Complexes of Cysteine, Histidine, and Derivatives Thereof: Potentiometric Determination of Their Compositions and Stabilities. *Helv. Chim. Acta 76*, 511−520.
(73) Vogler, R., and Vahrenkamp, H. (2002) Dipeptides Made up Solely from Histidine: Solution Behaviour and Zinc Complexation. *Eur. J. Inorg. Chem. 2002*, 761−766.
(74) Vallee, B. L., and Auld, D. S. (1993) Zinc: Biological Functions and Coordination Motifs. *Acc. Chem. Res. 26*, 543−551.
(75) Reddi, A. R., Guzman, T. R., Breece, R. M., Tierney, D. L., and Gibney, B. R. (2007) Deducing the Energetic Cost of Protein Folding in Zinc Finger Proteins Using Designed Metallopeptides. *J. Am. Chem. Soc. 129*, 12815−12827.
(76) Klemba, M., Gardner, K. H., Marino, S., Clarke, N. D., and Regan, L. (1995) Novel Metal-Binding Proteins by Design. *Nat. Struct. Biol. 2*, 368−373.
(77) Jacques, A., Mettra, B., Lebrun, V., Latour, J.-M., and Sénèque, O. (2013) On the Design of Zinc-Finger Models with Cyclic Peptides Bearing a Linear Tail. *Chemistry 19*, 3921−3931.
(78) Negi, S., Imanishi, M., Matsumoto, M., and Sugiura, Y. (2008) New Redesigned Zinc-Finger Proteins: Design Strategy and Its Application. *Chemistry 14*, 3236−3249.
(79) Mills, J. H., Khare, S. D., Bolduc, J. M., Forouhar, F., Mulligan, V. K., Lew, S., Seetharaman, J., Tong, L., Stoddard, B. L., and Baker, D. (2013) Computational Design of an Unnatural Amino Acid Dependent Metalloprotein with Atomic Level Accuracy. *J. Am. Chem. Soc. 135*, 13393−13399.
(80) Platt, G., Searle, M. S., and Chung, C.-W. (2001) Design of Histidine-Zn^{2+} Binding Sites Within a β-Hairpin Peptide: Enhancement of β-Sheet Stability through Metal Complexation. *Chem. Commun.*, 1162−1163.
(81) Imperiali, B., and Kapoor, T. M. (1993) The Reverse Turn as a Template for Metal Coordination. *Tetrahedron 49*, 3501−3510.
(82) Kiyokawa, T., Kanaori, K., Tajima, K., Koike, M., Mizuno, T., Oku, J.-I., and Tanaka, T. (2004) Binding of Cu(II) or Zn(II) in a de Novo Designed Triple-Stranded α-Helical Coiled-Coil Toward a Prototype for a Metalloenzyme. *J. Pept. Res. 63*, 347−353.
(83) Suzuki, K., Hiroaki, H., Kohda, D., Nakamura, H., and Tanaka, T. (1998) Metal Ion Induced Self-Assembly of a Designed Peptide into a Triple-Stranded α-Helical Bundle: A Novel Metal Binding Site in the Hydrophobic Core. *J. Am. Chem. Soc. 120*, 13008−13015.
(84) Wisz, M. S., Garrett, C. Z., and Hellinga, H. W. (1998) Construction of a Family of Cys_2His_2 Zinc Binding Sites in the Hydrophobic Core of Thioredoxin by Structure-Based Design. *Biochemistry 37*, 8269−8277.
(85) Zhu, C., Zhang, C., Liang, H., and Lai, L. (2011) Engineering a Zinc Binding Site into the de Novo Designed Protein DS119 with a B$\alpha\beta$ Structure. *Protein Cell 2*, 1006−1013.
(86) Reddi, A. R., and Gibney, B. R. (2007) Role of Protons in the Thermodynamic Contribution of a Zn(II)-Cys4 Site Toward Metalloprotein Stability. *Biochemistry 46*, 3745−3758.
(87) Petros, A. K., Reddi, A. R., Kennedy, M. L., Hyslop, A. G., and Gibney, B. R. (2006) Femtomolar Zn(II) Affinity in a Peptide-Based Ligand Designed to Model Thiolate-Rich Metalloprotein Active Sites. *Inorg. Chem. 45*, 9941−9958.
(88) Hellinga, H. W., and Richards, F. M. (1991) Construction of New Ligand Binding Sites in Proteins of Known Structure. I. Computer-Aided Modeling of Sites with Pre-Defined Geometry. *J. Mol. Biol. 222*, 763−785.
(89) Krizek, B. A., Merkle, D. L., and Berg, J. M. (1993) Ligand Variation and Metal Ion Binding Specificity in Zinc Finger Peptides. *Inorg. Chem. 32*, 937−940.
(90) Outten, C. E., and O'Halloran, T. V. (2001) Femtomolar Sensitivity of Metalloregulatory Proteins Controlling Zinc Homeostasis. *Science 292*, 2488−2492.
(91) Salgado, E. N., Radford, R. J., and Tezcan, F. A. (2010) Metal-Directed Protein Self-Assembly. *Acc. Chem. Res. 43*, 661−672.
(92) Radford, R. J., Brodin, J. D., Salgado, E. N., and Tezcan, F. A. (2011) Expanding the Utility of Proteins as Platforms for Coordination Chemistry. *Coord. Chem. Rev. 255*, 790−803.
(93) Matthews, J. M., Loughlin, F. E., and Mackay, J. P. (2008) Designed Metal-Binding Sites in Biomolecular and Bioinorganic Interactions. *Curr. Opin. Struct. Biol. 18*, 484−490.
(94) Brodin, J. D., Ambroggio, X. I., Tang, C., Parent, K. N., Baker, T. S., and Tezcan, F. A. (2012) Metal-Directed, Chemically Tunable Assembly of One-, Two- and Three-Dimensional Crystalline Protein Arrays. *Nat. Chem. 4*, 375−382.
(95) Der, B. S., Machius, M., Miley, M. J., Mills, J. L., Szyperski, T., and Kuhlman, B. (2012) Metal-Mediated Affinity and Orientation Specificity in a Computationally Designed Protein Homodimer. *J. Am. Chem. Soc. 134*, 375−385.
(96) Der, B. S., Edwards, D. R., and Kuhlman, B. (2012) Catalysis by a de Novo Zinc-Mediated Protein Interface: Implications for Natural Enzyme Evolution and Rational Enzyme Engineering. *Biochemistry 51*, 3933−3940.
(97) Salgado, E. N., Faraone-Mennella, J., and Tezcan, F. A. (2007) Controlling Protein-Protein Interactions through Metal Coordination: Assembly of a 16-Helix Bundle Protein. *J. Am. Chem. Soc. 129*, 13374−13375.
(98) Salgado, E. N., Lewis, R. A., Mossin, S., Rheingold, A. L., and Tezcan, F. A. (2009) Control of Protein Oligomerization Symmetry by

Metal Coordination: C2 and C3 Symmetrical Assemblies through Cu(II) and Ni(II) Coordination. *Inorg. Chem. 48*, 2726−2728.
(99) Liu, Y., and Kuhlman, B. (2006) RosettaDesign Server for Protein Design. *Nucleic Acids Res. 34*, W235−W238.
(100) Salgado, E. N., Ambroggio, X. I., Brodin, J. D., Lewis, R. A., Kuhlman, B., and Tezcan, F. A. (2010) Metal Templated Design of Protein Interfaces. *Proc. Natl. Acad. Sci. U.S.A. 107*, 1827−1832.
(101) Radford, R. J., Lawrenz, M., Nguyen, P. C., McCammon, J. A., and Tezcan, F. A. (2011) Porous Protein Frameworks with Unsaturated Metal Centers in Sterically Encumbered Coordination Sites. *Chem. Commun. 47*, 313−315.
(102) Medina-Morales, A., Perez, A., Brodin, J. D., and Tezcan, F. A. (2013) In Vitro and Cellular Self-Assembly of a Zn-Binding Protein Cryptand via Templated Disulfide Bonds. *J. Am. Chem. Soc. 135*, 12013−12022.
(103) Árus, D., Nagy, N. V., Dancs, Á., Jancsó, A., Berkecz, R., and Gajda, T. (2013) A Minimalist Chemical Model of Matrix Metalloproteinases: Can Small Peptides Mimic the More Rigid Metal Binding Sites of Proteins? *J. Inorg. Biochem. 126*, 61−69.
(104) Park, H.-S., Nam, S., Lee, J. K., Yoon, C. N., Mannervik, B., Benkovic, S. J., and Kim, H.-S. (2006) Design and Evolution of New Catalytic Activity with an Existing Protein Scaffold. *Science 311*, 535−538.
(105) Nomura, A., and Sugiura, Y. (2004) Hydrolytic Reaction by Zinc Finger Mutant Peptides: Successful Redesign of Structural Zinc Sites into Catalytic Zinc Sites. *Inorg. Chem. 43*, 1708−1713.
(106) Dhanasekaran, M., Negi, S., and Sugiura, Y. (2006) Designer Zinc Finger Proteins: Tools for Creating Artificial DNA-Binding Functional Proteins. *Acc. Chem. Res. 39*, 45−52.
(107) Higaki, J. N., Haymore, B. L., Chen, S., Fletterick, R. J., and Craik, C. S. (1990) Regulation of Serine Protease Activity by an Engineered Metal Switch. *Biochemistry 29*, 8582−8586.
(108) Halfon, S., and Craik, C. S. (1996) Regulation of Proteolytic Activity by Engineered Tridentate Metal Binding Loops. *J. Am. Chem. Soc. 118*, 1227−1228.
(109) Willett, W. S., Gillmor, S. A., Perona, J. J., Fletterick, R. J., and Craik, C. S. (1995) Engineered Metal Regulation of Trypsin Specificity. *Biochemistry 34*, 2172−2180.
(110) Willett, W. S., Brinen, L. S., Fletterick, R. J., and Craik, C. S. (1996) Delocalizing Trypsin Specificity with Metal Activation. *Biochemistry 35*, 5992−5998.
(111) Brinen, L. S., Willett, W. S., Craik, C. S., and Fletterick, R. J. (1996) X-Ray Structures of a Designed Binding Site in Trypsin Show Metal-Dependent Geometry. *Biochemistry 35*, 5999−6009.
(112) Jensen, K. K., Martini, L., and Schwartz, T. W. (2001) Enhanced Fluorescence Resonance Energy Transfer between Spectral Variants of Green Fluorescent Protein through Zinc-Site Engineering. *Biochemistry 40*, 938−945.
(113) Evers, T. H., Appelhof, M. A. M., de Graaf-Heuvelmans, P. T. H. M., Meijer, E. W., and Merkx, M. (2007) Ratiometric Detection of Zn(II) Using Chelating Fluorescent Protein Chimeras. *J. Mol. Biol. 374*, 411−425.
(114) Mizuno, T., Murao, K., Tanabe, Y., Oda, M., and Tanaka, T. (2007) Metal-Ion-Dependent GFP Emission in Vivo by Combining a Circularly Permutated Green Fluorescent Protein with an Engineered Metal-Ion-Binding Coiled-Coil. *J. Am. Chem. Soc. 129*, 11378−11383.
(115) Liu, H., Schmidt, J. J., Bachand, G. D., Rizk, S. S., Looger, L. L., Hellinga, H. W., and Montemagno, C. D. (2002) Control of a Biomolecular Motor-Powered Nanodevice with an Engineered Chemical Switch. *Nat. Mater. 1*, 173−177.
(116) Dwyer, M. A., Looger, L. L., and Hellinga, H. W. (2003) Computational Design of a Zn^{2+} Receptor That Controls Bacterial Gene Expression. *Proc. Natl. Acad. Sci. U.S.A. 100*, 11255−11260.
(117) Kiefer, L. L., and Fierke, C. A. (1994) Functional Characterization of Human Carbonic Anhydrase II Variants with Altered Zinc Binding Sites. *Biochemistry 33*, 15233−15240.
(118) Kiefer, L. L., Ippolito, J. A., Fierke, C. A., and Christianson, D. W. (1993) Redesigning the Zinc Binding Site of Human Carbonic Anhydrase II: Structure of a His_2Asp-Zn^{2+} Metal Coordination Polyhedron. *J. Am. Chem. Soc. 115*, 12581−12582.
(119) Song, H., Wilson, D. L., Farquhar, E. R., Lewis, E. A., and Emerson, J. P. (2012) Revisiting Zinc Coordination in Human Carbonic Anhydrase II. *Inorg. Chem. 51*, 11098−11105.
(120) Hunt, J. A., and Fierke, C. A. (1997) Selection of Carbonic Anhydrase Variants Displayed on Phage. Aromatic Residues in Zinc Binding Site Enhance Metal Affinity and Equilibration Kinetics. *J. Biol. Chem. 272*, 20364−20372.
(121) Alexander, R. S., Kiefer, L. L., Fierke, C. A., and Christianson, D. W. (1993) Engineering the Zinc Binding Site of Human Carbonic Anhydrase II: Structure of the His-94→Cys Apoenzyme in a New Crystalline Form. *Biochemistry 32*, 1510−1518.
(122) Ippolito, J. A., and Christianson, D. W. (1994) Structural Consequences of Redesigning a Protein-Zinc Binding Site. *Biochemistry 33*, 15241−15249.
(123) Ippolito, J. A., and Christianson, D. W. (1993) Structure of an Engineered His_3Cys Zinc Binding Site in Human Carbonic Anhydrase II. *Biochemistry 32*, 9901−9905.
(124) Ippolito, J. A., Baird, T. T., McGee, S. A., Christianson, D. W., and Fierke, C. A. (1995) Structure-Assisted Redesign of a Protein-Zinc-Binding Site with Femtomolar Affinity. *Proc. Natl. Acad. Sci. U.S.A. 92*, 5017−5021.
(125) Liang, Z., Xue, Y., Behravan, G., Jonsson, B. H., and Lindskog, S. (1993) Importance of the Conserved Active-Site Residues Tyr7, Glu106 and Thr199 for the Catalytic Function of Human Carbonic Anhydrase II. *Eur. J. Biochem. 211*, 821−827.
(126) Krebs, J. F., Fierke, C. A., Alexander, R. S., and Christianson, D. W. (1991) Conformational Mobility of His-64 in the Thr-200 → Ser Mutant of Human Carbonic Anhydrase II. *Biochemistry 30*, 9153−9160.
(127) Kiefer, L. L., Paterno, S. A., and Fierke, C. A. (1995) Hydrogen Bond Network in the Metal Binding Site of Carbonic Anhydrase Enhances Zinc Affinity and Catalytic Efficiency. *J. Am. Chem. Soc. 117*, 6831−6837.
(128) Lesburg, C. A., and Christianson, D. W. (1995) X-ray Crystallographic Studies of Engineered Hydrogen Bond Networks in a Protein-Zinc Binding Site. *J. Am. Chem. Soc. 117*, 6838−6844.
(129) Huang, C. C., Lesburg, C. A., Kiefer, L. L., Fierke, C. A., and Christianson, D. W. (1996) Reversal of the Hydrogen Bond to Zinc Ligand Histidine-119 Dramatically Diminishes Catalysis and Enhances Metal Equilibration Kinetics in Carbonic Anhydrase II. *Biochemistry 35*, 3439−3446.
(130) Elleby, B., Sjöblom, B., and Lindskog, S. (1999) Changing the Efficiency and Specificity of the Esterase Activity of Human Carbonic Anhydrase II by Site-Specific Mutagenesis. *Eur. J. Biochem. 262*, 516−521.
(131) Höst, G., Mårtensson, L.-G., and Jonsson, B.-H. (2006) Redesign of Human Carbonic Anhydrase II for Increased Esterase Activity and Specificity Towards Esters with Long Acyl Chains. *Biochim. Biophys. Acta 1764*, 1601−1606.
(132) Höst, G. E., and Jonsson, B.-H. (2008) Converting Human Carbonic Anhydrase II into a Benzoate Ester Hydrolase through Rational Redesign. *Biochim. Biophys. Acta 1784*, 811−815.
(133) Tallant, C., Marrero, A., and Gomis-Rüth, F. X. (2010) Matrix Metalloproteinases: Fold and Function of Their Catalytic Domains. *Biochim. Biophys. Acta 1803*, 20−28.
(134) Kimura, E., Shiota, T., Koike, T., Shiro, M., and Kodama, M. (1990) A Zinc(II) Complex of 1,5,9-Triazacyclododecane ([12]-aneN3) as a Model for Carbonic Anhydrase. *J. Am. Chem. Soc. 112*, 5805−5811.
(135) Koerner, T. B., and Brown, R. S. (2002) The Hydrolysis of an Activated Ester by a Tris(4,5-di-n-propyl-2-imidazolyl)phosphine-Zn^{2+} Complex in Neutral Micellar Medium as a Model for Carbonic Anhydrase. *Can. J. Chem. 80*, 183−191.
(136) Bazzicalupi, C., Bencini, A., Bianchi, A., Fusi, V., Giorgi, C., Paoletti, P., Valtancoli, B., and Zanchi, D. (1997) Carboxy and Phosphate Esters Cleavage with Mono- and Dinuclear Zinc(II) Macrocyclic Complexes in Aqueous Solution. Crystal Structure of

$[Zn_2L1(\mu\text{-}PP)_2(MeOH)_2](ClO_4)_2$ (L1 = [30]aneN6O4, PP- = Diphenyl Phosphate). *Inorg. Chem. 36*, 2784−2790.
(137) Cameron, A. D., Ridderström, M., Olin, B., and Mannervik, B. (1999) Crystal Structure of Human Glyoxalase II and Its Complex with a Glutathione Thiolester Substrate Analogue. *Structure 7*, 1067−1078.
(138) Wang, Z., Fast, W., Valentine, A. M., and Benkovic, S. J. (1999) Metallo-β-Lactamase: Structure and Mechanism. *Curr. Opin. Chem. Biol. 3*, 614−622.
(139) Lombardi, A., Summa, C. M., Geremia, S., Randaccio, L., Pavone, V., and DeGrado, W. F. (2000) Retrostructural Analysis of Metalloproteins: Application to the Design of a Minimal Model for Diiron Proteins. *Proc. Natl. Acad. Sci. U.S.A. 97*, 6298−6305.
(140) Merkle, D. L., Schmidt, M. H., and Berg, J. M. (1991) Design and Characterization of a Ligand-Binding Metallopeptide. *J. Am. Chem. Soc. 113*, 5450−5451.
(141) Nomura, A., and Sugiura, Y. (2002) Contribution of Individual Zinc Ligands to Metal Binding and Peptide Folding of Zinc Finger Peptides. *Inorg. Chem. 41*, 3693−3698.
(142) Negi, S., Itazu, M., Imanishi, M., Nomura, A., and Sugiura, Y. (2004) Creation and Characteristics of Unnatural $CysHis_3$-Type Zinc Finger Protein. *Biochem. Biophys. Res. Commun. 325*, 421−425.
(143) Itoh, T., Fujii, Y., Tada, T., Yoshikawa, Y., and Hisada, H. (1996) Thermodynamic and Kinetic Studies of Zinc(II)-Triamine Complexes as Models of CA and AP. *Bull. Chem. Soc. Jpn. 69*, 1265−1274.
(144) King, D. A., Zhang, L., Guarente, L., and Marmorstein, R. (1999) Structure of a HAP1-DNA Complex Reveals Dramatically Asymmetric DNA Binding by a Homodimeric Protein. *Nat. Struct. Biol. 6*, 64−71.
(145) Hori, Y., Suzuki, K., Okuno, Y., Nagaoka, M., Futaki, S., and Sugiura, Y. (2000) Artificial Zinc Finger Peptide Containing a Novel His4 Domain. *J. Am. Chem. Soc. 122*, 7648−7653.
(146) Salgado, E. N., Lewis, R. A., Faraone-Mennella, J., and Tezcan, F. A. (2008) Metal-Mediated Self-Assembly of Protein Superstructures: Influence of Secondary Interactions on Protein Oligomerization and Aggregation. *J. Am. Chem. Soc. 130*, 6082−6084.
(147) Koike, T., Takamura, M., and Kimura, E. (1994) Role of Zinc(II) in β-Lactamase II: A Model Study with a Zinc(II)-Macrocyclic Tetraamine (1,4,7,10-Tetraazacyclododecane, Cyclen) Complex. *J. Am. Chem. Soc. 116*, 8443−8449.
(148) Kimura, E., Hashimoto, H., and Koike, T. (1996) Hydrolysis of Lipophilic Esters Catalyzed by a Zinc(II) Complex of a Long Alkyl-Pendant Macrocyclic Tetraamine in Micellar Solution. *J. Am. Chem. Soc. 118*, 10963−10970.
(149) Innocenti, A., Scozzafava, A., Parkkila, S., Puccetti, L., De Simone, G., and Supuran, C. T. (2008) Investigations of the Esterase, Phosphatase, and Sulfatase Activities of the Cytosolic Mammalian Carbonic Anhydrase Isoforms I, II, and XIII with 4-Nitrophenyl Esters as Substrates. *Bioorg. Med. Chem. Lett. 18*, 2267−2271.
(150) Nomura, A., and Sugiura, Y. (2004) Sequence-Selective and Hydrolytic Cleavage of DNA by Zinc Finger Mutants. *J. Am. Chem. Soc. 126*, 15374−15375.
(151) Patel, K., Srivastava, K. R., and Durani, S. (2010) Zinc-Finger Hydrolase: Computational Selection of a Linker and a Sequence Towards Metal Activation with a Synthetic A$\beta\beta$ Protein. *Bioorg. Med. Chem. 18*, 8270−8276.
(152) Zastrow, M. L., Peacock, A. F. A., Stuckey, J. A., and Pecoraro, V. L. (2012) Hydrolytic Catalysis and Structural Stabilization in a Designed Metalloprotein. *Nat. Chem. 4*, 118−123.
(153) Khare, S. D., Kipnis, Y., Greisen, P. J., Takeuchi, R., Ashani, Y., Goldsmith, M., Song, Y., Gallaher, J. L., Silman, I., Leader, H., et al. (2012) Computational Redesign of a Mononuclear Zinc Metalloenzyme for Organophosphate Hydrolysis. *Nat. Chem. Biol. 8*, 294−300.
(154) Dieckmann, G. R., McRorie, D. K., Tierney, D. L., Utschig, L. M., Singer, C. P., O'Halloran, T. V., Penner-Hahn, J. E., DeGrado, W. F., and Pecoraro, V. L. (1997) De Novo Design of Mercury-Binding Two- and Three-Helical Bundles. *J. Am. Chem. Soc. 119*, 6195−6196.
(155) Dieckmann, G. R., McRorie, D. K., Lear, J. D., Sharp, K. A., DeGrado, W. F., and Pecoraro, V. L. (1998) The Role of Protonation and Metal Chelation Preferences in Defining the Properties of Mercury-Binding Coiled Coils. *J. Mol. Biol. 280*, 897−912.
(156) Farrer, B. T., and Pecoraro, V. L. (2003) Hg(II) Binding to a Weakly Associated Coiled Coil Nucleates an Encoded Metalloprotein Fold: A Kinetic Analysis. *Proc. Natl. Acad. Sci. U.S.A. 100*, 3760−3765.
(157) Farrer, B. T., Harris, N. P., Balchus, K. E., and Pecoraro, V. L. (2001) Thermodynamic Model for the Stabilization of Trigonal Thiolato Mercury(II) in Designed Three-Stranded Coiled Coils. *Biochemistry 40*, 14696−14705.
(158) Matzapetakis, M., Farrer, B. T., Weng, T.-C., Hemmingsen, L., Penner-Hahn, J. E., and Pecoraro, V. L. (2002) Comparison of the Binding of Cadmium(II), Mercury(II), and Arsenic(III) to the de Novo Designed Peptides TRI L12C and TRI L16C. *J. Am. Chem. Soc. 124*, 8042−8054.
(159) Łuczkowski, M., Stachura, M., Schirf, V., Demeler, B., Hemmingsen, L., and Pecoraro, V. L. (2008) Design of Thiolate Rich Metal Binding Sites Within a Peptidic Framework. *Inorg. Chem. 47*, 10875−10888.
(160) Iranzo, O., Thulstrup, P. W., Ryu, S.-B., Hemmingsen, L., and Pecoraro, V. L. (2007) The Application of ^{199}Hg NMR and ^{199m}Hg Perturbed Angular Correlation (PAC) Spectroscopy to Define the Biological Chemistry of Hg(II): A Case Study with Designed Two- and Three-Stranded Coiled Coils. *Chemistry 13*, 9178−9190.
(161) Dieckmann, G. (1995) Use of Metal-Binding de Novo-Designed α-Helical Peptides in the Study of Metalloprotein Structures. Ph.D. Thesis, University of Michigan, Ann Arbor, MI.
(162) Ghosh, D., and Pecoraro, V. L. (2004) Understanding Metalloprotein Folding Using a de Novo Design Strategy. *Inorg. Chem. 43*, 7902−7915.
(163) Pecoraro, V. L., Peacock, A. F. A., Iranzo, O., and Luczkowski, M. (2009) Understanding the Biological Chemistry of Mercury Using a de Novo Protein Design Strategy. *ACS Symp. Ser. 1012*, 183−197.
(164) Iranzo, O., Ghosh, D., and Pecoraro, V. L. (2006) Assessing the Integrity of Designed Homomeric Parallel Three-Stranded Coiled Coils in the Presence of Metal Ions. *Inorg. Chem. 45*, 9959−9973.
(165) Rulíšek, L., and Vondràšek, J. (1998) Coordination Geometries of Selected Transition Metal Ions (Co^{2+}, Ni^{2+}, Cu^{2+}, Zn^{2+}, Cd^{2+}, and Hg^{2+}) in Metalloproteins. *J. Inorg. Biochem. 71*, 115−127.
(166) Zheng, H., Chruszcz, M., Lasota, P., Lebioda, L., and Minor, W. (2008) Data Mining of Metal Ion Environments Present in Protein Structures. *J. Inorg. Biochem. 102*, 1765−1776.
(167) Wright, J. G., Tsang, H. T., Penner-Hahn, J. E., and O'Halloran, T. V. (1990) Coordination Chemistry of the Hg-MerR Metalloregulatory Protein: Evidence for a Novel Tridentate Mercury-Cysteine Receptor Site. *J. Am. Chem. Soc. 112*, 2434−2435.
(168) Zastrow, M. L., and Pecoraro, V. L. (2013) Influence of Active Site Location on Catalytic Activity in de Novo-Designed Zinc Metalloenzymes. *J. Am. Chem. Soc. 135*, 5895−5903.
(169) Krebs, J. F., Ippolito, J. A., Christianson, D. W., and Fierke, C. A. (1993) Structural and Functional Importance of a Conserved Hydrogen Bond Network in Human Carbonic Anhydrase II. *J. Biol. Chem. 268*, 27458−27466.
(170) Pocker, Y., and Stone, J. T. (1968) The Catalytic Versatility of Erythrocyte Carbonic Anhydrase. VI. Kinetic Studies of Non-competitive Inhibition of Enzyme-Catalyzed Hydrolysis of p-Nitrophenyl Acetate. *Biochemistry 7*, 2936−2945.
(171) Pocker, Y., and Deits, T. L. (1982) Effects of pH on Anionic Inhibition of Carbonic Anhydrase Activities. *J. Am. Chem. Soc. 104*, 2424−2434.
(172) Pocker, Y., and Stone, J. T. (1967) The Catalytic Versatility of Erythrocyte Carbonic Anhydrase. III. Kinetic Studies of the Enzyme-Catalyzed Hydrolysis of p-Nitrophenyl Acetate. *Biochemistry 6*, 668−678.
(173) Gomez-Tagle, P., Vargas-Zúñiga, I., Taran, O., and Yatsimirsky, A. K. (2006) Solvent Effects and Alkali Metal Ion Catalysis in Phosphodiester Hydrolysis. *J. Org. Chem. 71*, 9713−9722.

(174) Woolley, P. (1975) Models for Metal Ion Function in Carbonic Anhydrase. *Nature 258*, 677−682.
(175) Huguet, J., and Brown, R. S. (1980) Catalytically Active Models for the Active Site in Carbonic Anhydrase. *J. Am. Chem. Soc. 102*, 7571−7572.
(176) Brown, R. S., Curtis, N. J., and Huguet, J. (1981) Tris(4,5-diisopropylimidazol-2-yl)phosphine:zinc^{2+}. A Catalytically Active Model for Carbonic Anhydrase. *J. Am. Chem. Soc. 103*, 6953−6959.
(177) Brown, R. S., Salmon, D., Curtis, N. J., and Kusuma, S. (1982) Carbonic Anhydrase Models. 4. [Tris[(4,5-dimethyl-2-imidazolyl)-methyl]phosphine oxide]cobalt^{2+}, a Small-Molecule Mimic of the Spectroscopic Properties of Cobalt(II) Carbonic Anhydrase. *J. Am. Chem. Soc. 104*, 3188−3194.
(178) Slebocka-Tilk, H., Cocho, J. L., Frackman, Z., and Brown, R. S. (1984) Carbonic Anhydrase Models. 5. Tris(4,5-di-n-propyl-2-imidazolyl)phosphine-zinc^{2+} and Bis(4,5-di-isopropyl-2-imidazolyl)-2-imidazolylphosphine-zinc^{2+}. Catalysts Facilitating Hydrogen Carbonate to Carbon Dioxide (HCO_3^- to CO_2) Interconversion. *J. Am. Chem. Soc. 106*, 2421−2431.
(179) Zhang, X., van Eldik, R., Koike, T., and Kimura, E. (1993) Kinetics and Mechanism of the Hydration of Carbon Dioxide and Dehydration of Bicarbonate Catalyzed by a Zinc(II) Complex of 1,5,9-Triazacyclododecane as a Model for Carbonic Anhydrase. *Inorg. Chem. 32*, 5749−5755.
(180) Zhang, X., and van Eldik, R. (1995) A Functional Model for Carbonic Anhydrase: Thermodynamic and Kinetic Study of a Tetraazacyclododecane Complex of Zinc(II). *Inorg. Chem. 34*, 5606−5614.
(181) Nakata, K., Shimomura, N., Shiina, N., Izumi, M., Ichikawa, K., and Shiro, M. (2002) Kinetic Study of Catalytic CO_2 Hydration by Water-Soluble Model Compound of Carbonic Anhydrase and Anion Inhibition Effect on CO_2 Hydration. *J. Inorg. Biochem. 89*, 255−266.
(182) Supuran, C. T. (2008) Carbonic Anhydrases: An Overview. *Curr. Pharm. Des. 14*, 603−614.
(183) Benson, D. E., Wisz, M. S., and Hellinga, H. W. (2000) Rational Design of Nascent Metalloenzymes. *Proc. Natl. Acad. Sci. U.S.A. 97*, 6292−6297.
(184) Chakraborty, S., Touw, D. S., Peacock, A. F. A., Stuckey, J., and Pecoraro, V. L. (2010) Structural Comparisons of Apo- and Metalated Three-Stranded Coiled Coils Clarify Metal Binding Determinants in Thiolate Containing Designed Peptides. *J. Am. Chem. Soc. 132*, 13240−13250.
(185) Matzapetakis, M., Ghosh, D., Weng, T.-C., Penner-Hahn, J. E., and Pecoraro, V. L. (2006) Peptidic Models for the Binding of Pb(II), Bi(III) and Cd(II) to Mononuclear Thiolate Binding Sites. *JBIC, J. Biol. Inorg. Chem. 11*, 876−890.
(186) Fierke, C. A., Calderone, T. L., and Krebs, J. F. (1991) Functional Consequences of Engineering the Hydrophobic Pocket of Carbonic Anhydrase II. *Biochemistry 30*, 11054−11063.
(187) Marino, S. F., and Regan, L. (1999) Secondary Ligands Enhance Affinity at a Designed Metal-Binding Site. *Chem. Biol. 6*, 649−655.
(188) Prigge, S. T., Kolhekar, A. S., Eipper, B. A., Mains, R. E., and Amzel, L. M. (1997) Amidation of Bioactive Peptides: The Structure of Peptidylglycine α-Hydroxylating Monooxygenase. *Science 278*, 1300−1305.
(189) Jacobson, F., Pistorius, A., Farkas, D., De Grip, W., Hansson, O., Sjölin, L., and Neutze, R. (2007) pH Dependence of Copper Geometry, Reduction Potential, and Nitrite Affinity in Nitrite Reductase. *J. Biol. Chem. 282*, 6347−6355.
(190) Johnson, B. J., Cohen, J., Welford, R. W., Pearson, A. R., Schulten, K., Klinman, J. P., and Wilmot, C. M. (2007) Exploring Molecular Oxygen Pathways in Hansenula Polymorpha Copper-Containing Amine Oxidase. *J. Biol. Chem. 282*, 17767−17776.
(191) Fusetti, F., Schröter, K. H., Steiner, R. A., van Noort, P. I., Pijning, T., Rozeboom, H. J., Kalk, K. H., Egmond, M. R., and Dijkstra, B. W. (2002) Crystal Structure of the Copper-Containing Quercetin 2,3-Dioxygenase from *Aspergillus japonicus*. *Structure 10*, 259−268.
(192) Tegoni, M., Yu, F., Bersellini, M., Penner-Hahn, J. E., and Pecoraro, V. L. (2012) Designing a Functional Type 2 Copper Center That Has Nitrite Reductase Activity Within α-Helical Coiled Coils. *Proc. Natl. Acad. Sci. U.S.A. 109*, 21234−21239.
(193) Gomis-Rüth, F. X., Kress, L. F., and Bode, W. (1993) First Structure of a Snake Venom Metalloproteinase: A Prototype for Matrix Metalloproteinases/Collagenases. *EMBO J. 12*, 4151−4157.
(194) Touw, D. S., Nordman, C. E., Stuckey, J. A., and Pecoraro, V. L. (2007) Identifying Important Structural Characteristics of Arsenic Resistance Proteins by Using Designed Three-Stranded Coiled Coils. *Proc. Natl. Acad. Sci. U.S.A. 104*, 11969−11974.
(195) Holm, R. H., Kennepohl, P., and Solomon, E. I. (1996) Structural and Functional Aspects of Metal Sites in Biology. *Chem. Rev. 96*, 2239−2314.
(196) *The PyMOL Molecular Graphics System*, version 1.5.0.4, Schrödinger, LLC, Portland, OR, 2010.